GEOTHERMAL EXPLORATION OF THE MENENGAI GEOTHERMAL FIELD

Geoffrey Mibei
Geothermal Development Company
P.O. Box 17700-20100, Nakuru
KENYA
gmibei@gdc.co.ke

ABSTRACT

In geothermal resource assessment a multidisciplinary approach is adopted. The aim is to ascertain and map the size of the reservoir, determine reservoir temperature and chemical composition of the reservoir fluids. Ultimately, a conceptual model and sites for exploration drilling are produced. This paper describes findings and current status of Menengai geothermal exploration and resource assessment respectively. Deep drilling geothermal program in Menengai field has so far resulted in 31 geothermal wells within the Menengai Caldera. Geoscientific data acquired are continually reviewed and integrated to bring out an updated geothermal model of the field. Current geoscientific data shows that Menengai caldera has been volcanically active in recent geological time. In regards to fluid flow, the most significant structures are mainly the young NNE-SSW, this based on measured temperature contours. Other regional structures are those oriented to N-S and E-W. The N-S are older regional structures while the E-W are local structures are as a result of near field stresses related to magma uplifting within the centre of the caldera. Assessment from the surface geology indicates that the most active area is the central (summit) and south of caldera owing to young structures and widespread eruption. Borehole geology data shows that a syn-caldera tuff marker horizon between 300-400 m CT is present in all wells. Moreover high temperature alteration minerals like actinolite are present in wells drilled within the summit area indicating zones of contact metamorphism related to system of hot dike intrusions. These dike systems can also be inferred from surface data that shows a majority of lava eruption are within the summit area. In addition syenitic intrusive have been encountered from the wells within the caldera summit area as deduced from borehole geology data and measured temperature. Measured temperature contours shows a marked NNE-SSW anomaly pattern inferring fluid flow pattern. Gravity survey presents an anomaly at the centre of the caldera which is most likely related to a magmatic forming the dike intrusion. Furthermore, the aforementioned summit area exhibits shallow seismic movements confirming shallow magmatic activity. Resistivity interpretations have some ambiguity but it is certain that the reservoir is around 30ohm-m. The discharge chemistry of wells shows that the discharge is Na-HCO3 fluid with a high pH and moderately high chloride concentrations (> 400 mg/kg). The reservoir fluids exhibit marked variations whereby some wells discharge one phase (i.e. steam) while the others discharge two phase. It can be concluded from the fluid and gas chemistry of the discharged wells and temperature contours, it is evident that the wells around the small portion of the summit area is within the up-flow thus displaying low NCG contents, low CO_2 and high temperature

1. INTRODUCTION

The Menengai geothermal field hosts one of the high-temperature geothermal systems in Kenya. It is located in Nakuru within the central Kenyan Rift Valley (Figure 1) and comprises the Menengai caldera, The Ol'rongai in the northwest and parts of the Solai graben to the northeast.
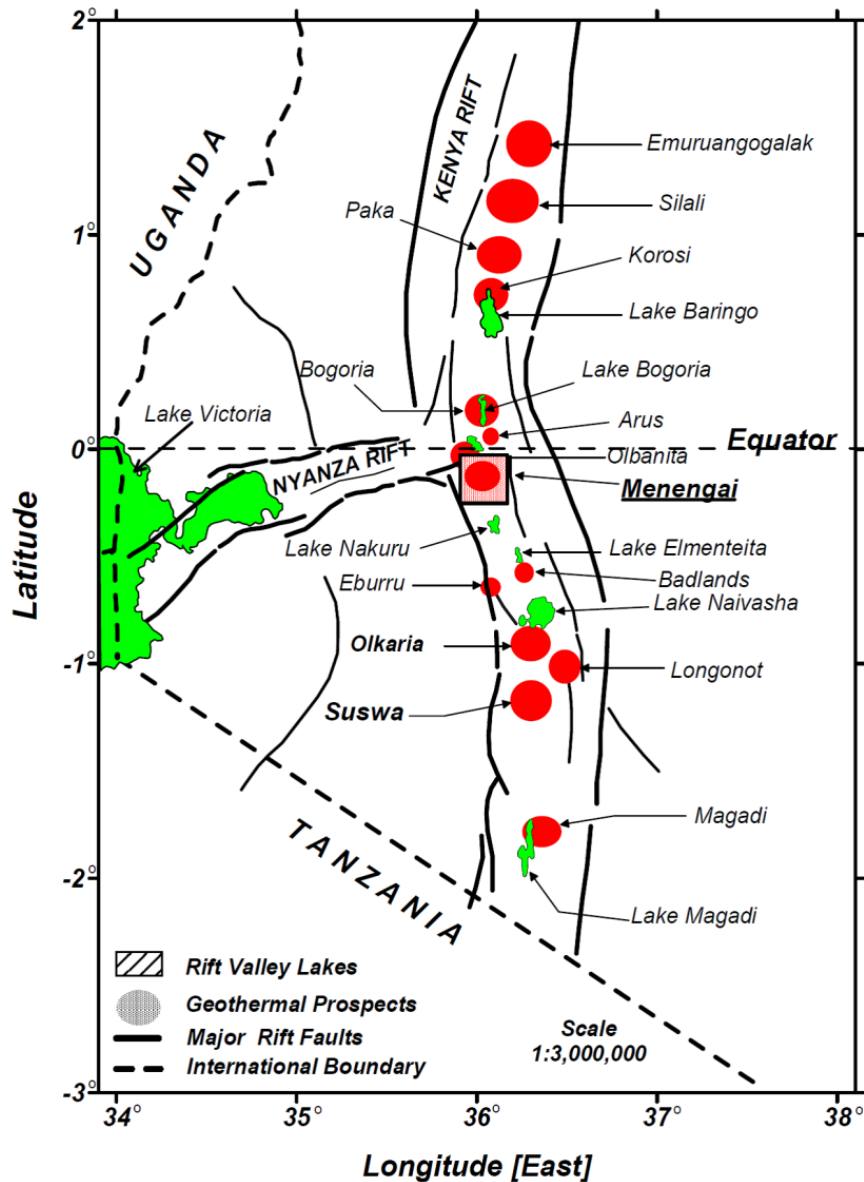

FIGURE 1: Location of the Menengai field within the Kenyan Rift Valley (Simiyu, 2009)

2. GEOLOGY

2.1 Surface geology

Generally the geological units exposed in Menengai area include; Menengai pyroclastic, Ol'rongai pyroclastic, Ol'Banita volcanics, Ol'rongai volcanics, Menengai ignimbrites, Solai tuffs, rumuruti phonolites and the Menengai lavas (Figure 2). The lithological units can be grouped by relative ages of the Menengai pre-caldera, Menengai syn-caldera and Menengai post caldera. Based on this grouping the youngest to oldest lithological units are alluvial deposits, Menengai caldera lavas, Ol'rongai

volcanic, Ol'Banita volcanic, Ol'rongai pyroclastic, Menengai pyroclastic, Solai tuffs while the oldest are Rumuruti phonolites.
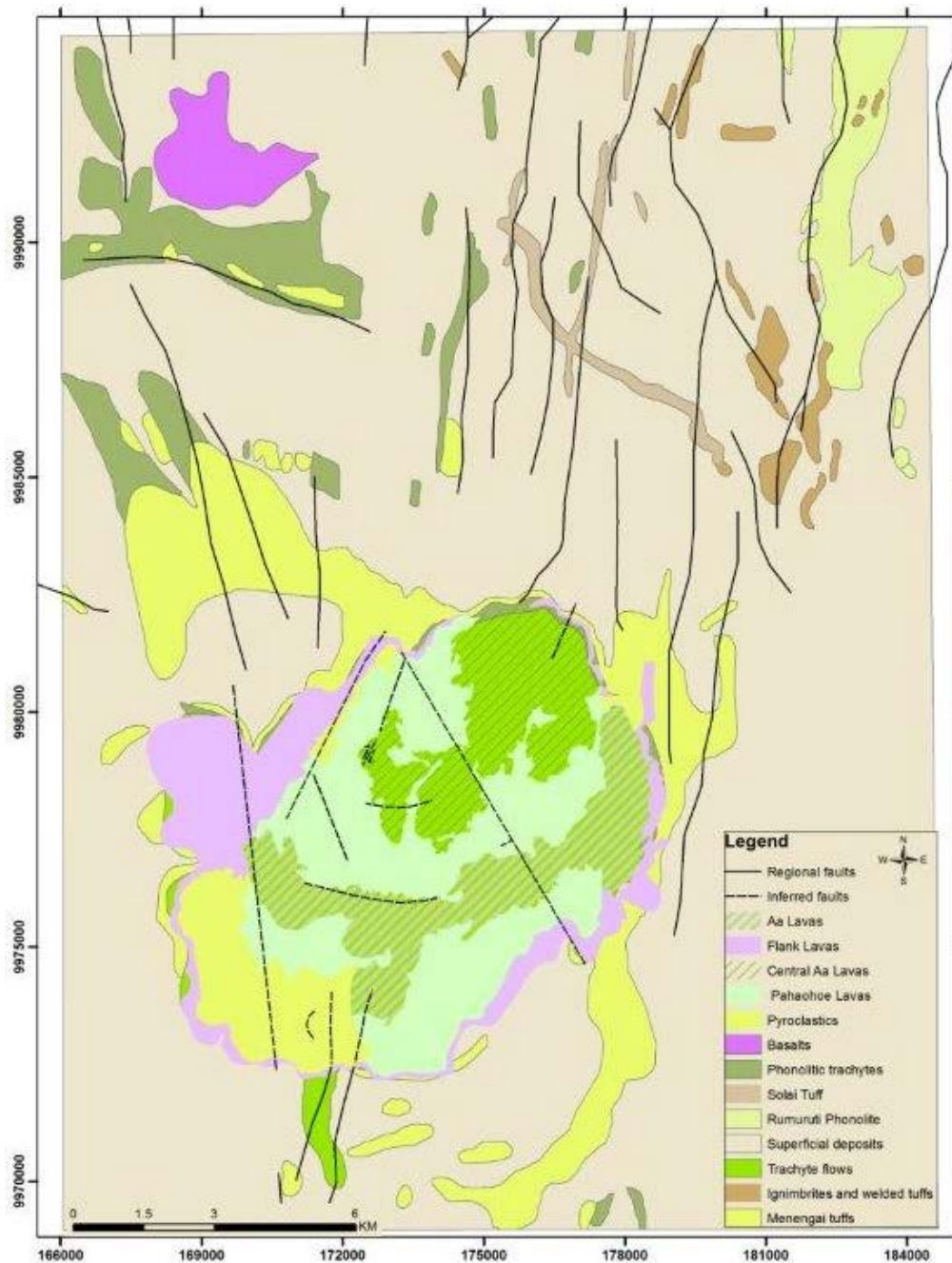

FIGURE 2: Geological map of Menengai geothermal prospect (modified from Robinson, 2015)

2.1.1 Menengai caldera

The surface geology of the Menengai caldera is dominated by trachyte lavas with variations in textural and flow characteristic, pyroclastic, ignimbrites and basalts are also present. The youngest eruption lava flows are located at the centre of the caldera with a smaller flow to the south. The youngest flows are traced to the fissures in an E-W orientation inferring a recent fault activity. Preponderance of the pyroclastics are to the west probably due to a prevailing easterly winds at the time of the eruption. The most productive wells are within the centre and area of recent activity. Areas of exploration and

expansion could be to the south and northeast where both young faults and eruptive activity are palpable (Figure 3).
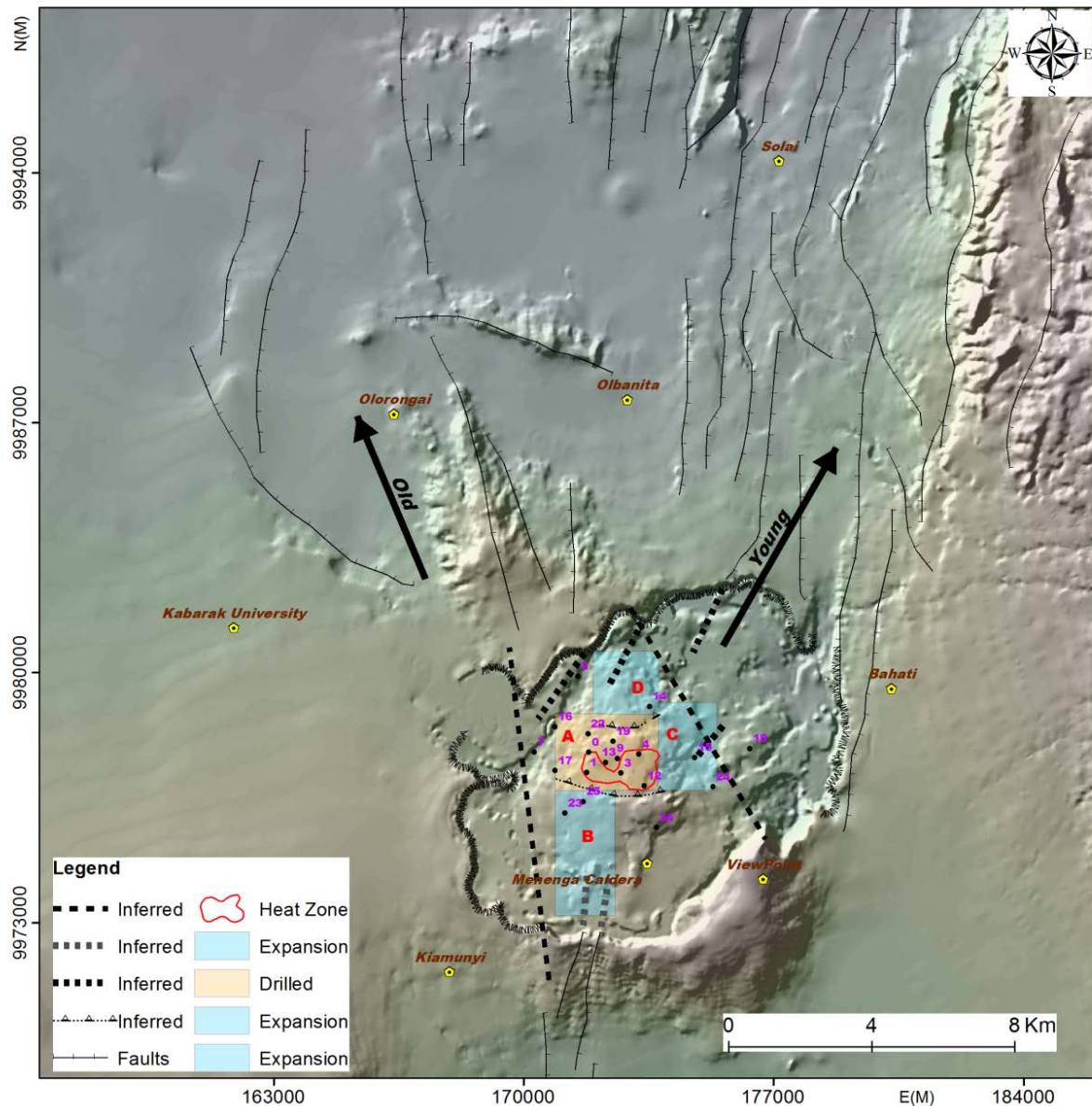

FIGURE 3: Map of areas of recent geologic activity and possible expansion zones

2.1.2 Regional structures

The general trend of many structures within Menengai area prospect is NNE-SSW in the east and N-S in the central and NNW-SSE in western zone (Figure 4). The NNE-SSW normal fault forms the Solai half graben, These structures are younger than the caldera and cuts through the caldera rim in the northeast, they extends further northwards up to Lake Bogoria where most hot springs occur. They probably were also control the caldera formation as the caldera is orientated in an NNE orientation. The N-S and NNW-SSE are older than the NNE-SSW faults. the N-S trending faults constitutes the Molo graben constitutes to the north of caldera and it is within this narrow graben that the fault controlled Arus steam jets, Arus fumaroles north of Ol 'rongai occurs. The NNW-SSE constitute the Ol' rongai ridge, where geothermal manifestations inform of hot altered ground and travertine depositions are present. The boreholes immediately to the north and northwest of the Menengai caldera show lake water

contamination indicating interconnection with Lake Nakuru system (Geotermica Italiana Srl, 1987) inferring permeability and interconnection between the lake Nakuru on the south and northern region of Menengai made possible by these older N-S and NNW-SSE faults. The Ol'Banita swamp is located in an area dominated by dry and thermally anomalous boreholes. The productive ones are characterized by very shallow, low-yield aquifers that get depleted fast since the deeper formations are impervious. The swamp owes its existence to impervious bedrocks that have been affected by hydrothermal alteration. This shows that this structure could be of great significance for the geothermal system with Menengai area.
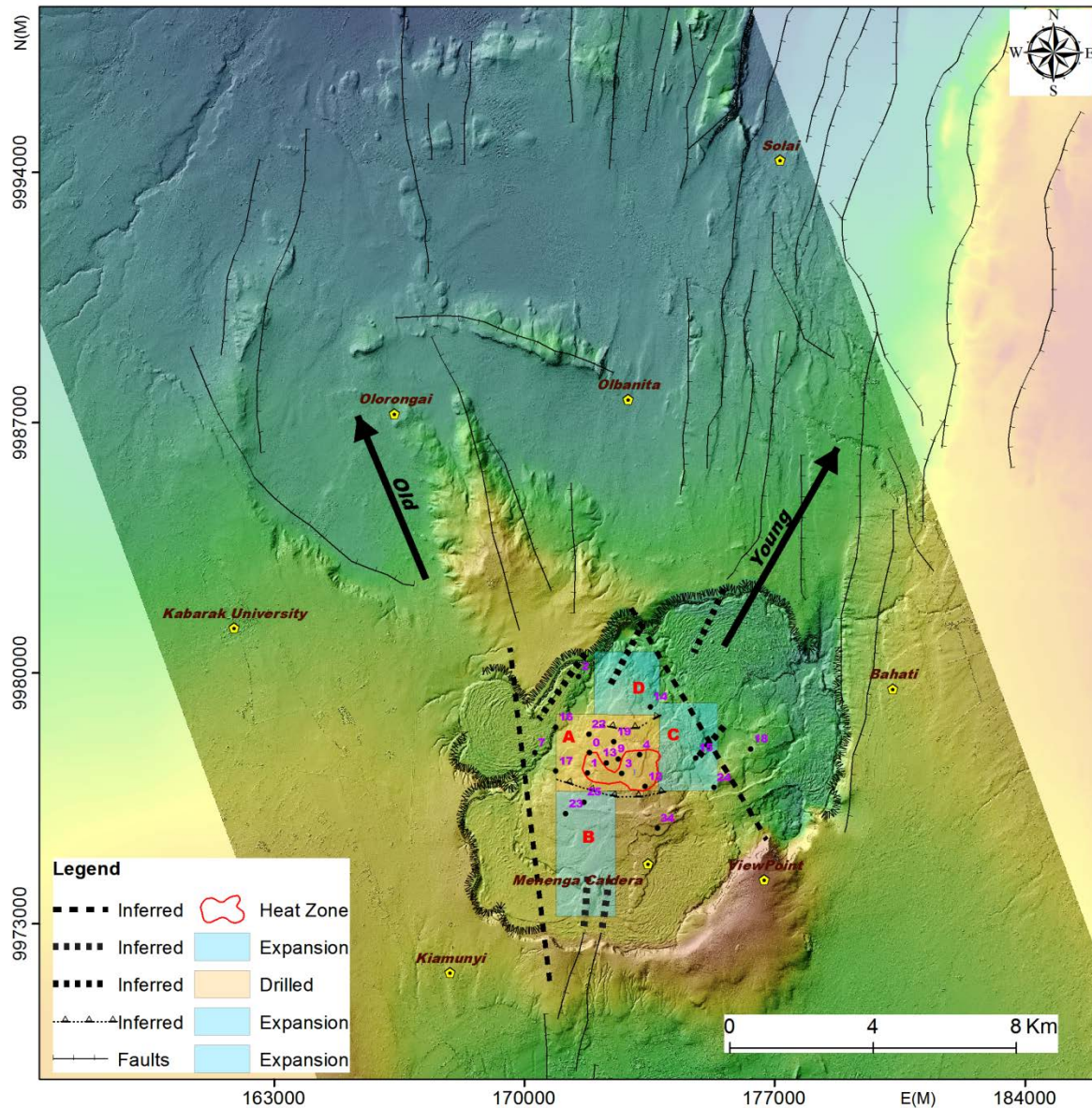

FIGURE 4: Regional structural setting

2.1.3 Local structures

In a local scale Menengai caldera (Figure 5) appears to have cut through a pre-existing NNW-SSE "ridge structure" probably associated with the primitive shield caldera. Observations of already drilled wells shows that the most successful well are within this ridge boundaries meaning that the ridge is structural control of some sort for the system however fluid flow is impacted majorly by the young structures NNE-SSW. The E-W structures related to near field stress of magmatic influence may have local

influence on the geothermal system. The fumarole and altered grounds are located at the central part of the caldera, northwest and north. Other important features of geothermal significance are found in the south where very young structures manifest including young eruptive event of a lava flow from the outer southern part of the caldera into the inner Calder region. This regions are therefore every interesting and could potentially be a resourceful area from a geological perspective.
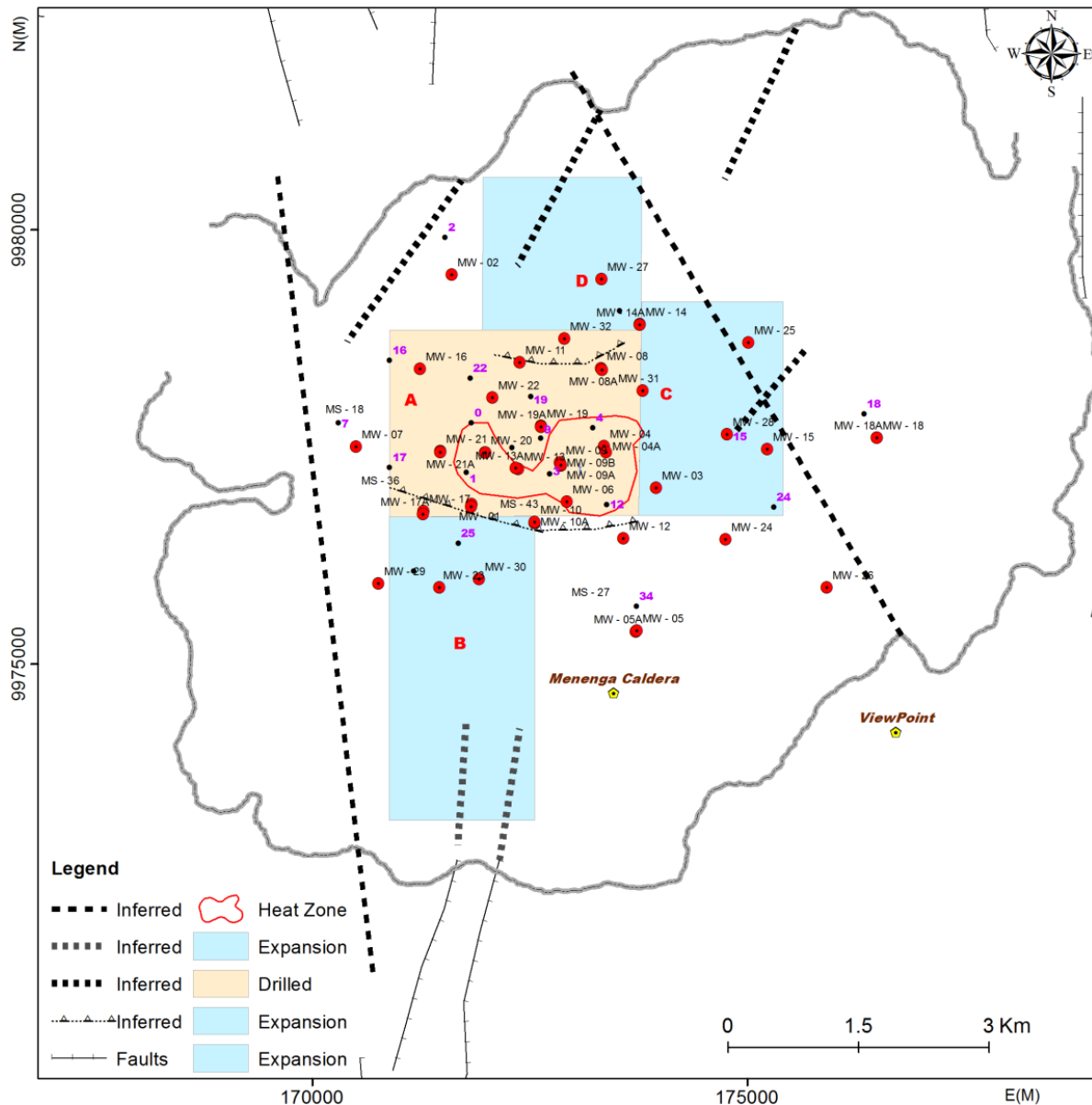

FIGURE 5: Menengai caldera local structures

2.2 Borehole geology

2.2.1 Lithostratigraphy

The stratigraphy of Menengai (Figure 6) is complex however what is clear is that at least one marker horizons is present at 300-400 m CT (Mibei 2012). Based on current borehole geology data the top of the shield volcano can be clearly outlined, i.e. the boundary of pre-caldera and the post caldera volcanics. Magma has been encountered slightly below 2 km within summit area. This is an area of stress transfer where fissure swamps may be present.
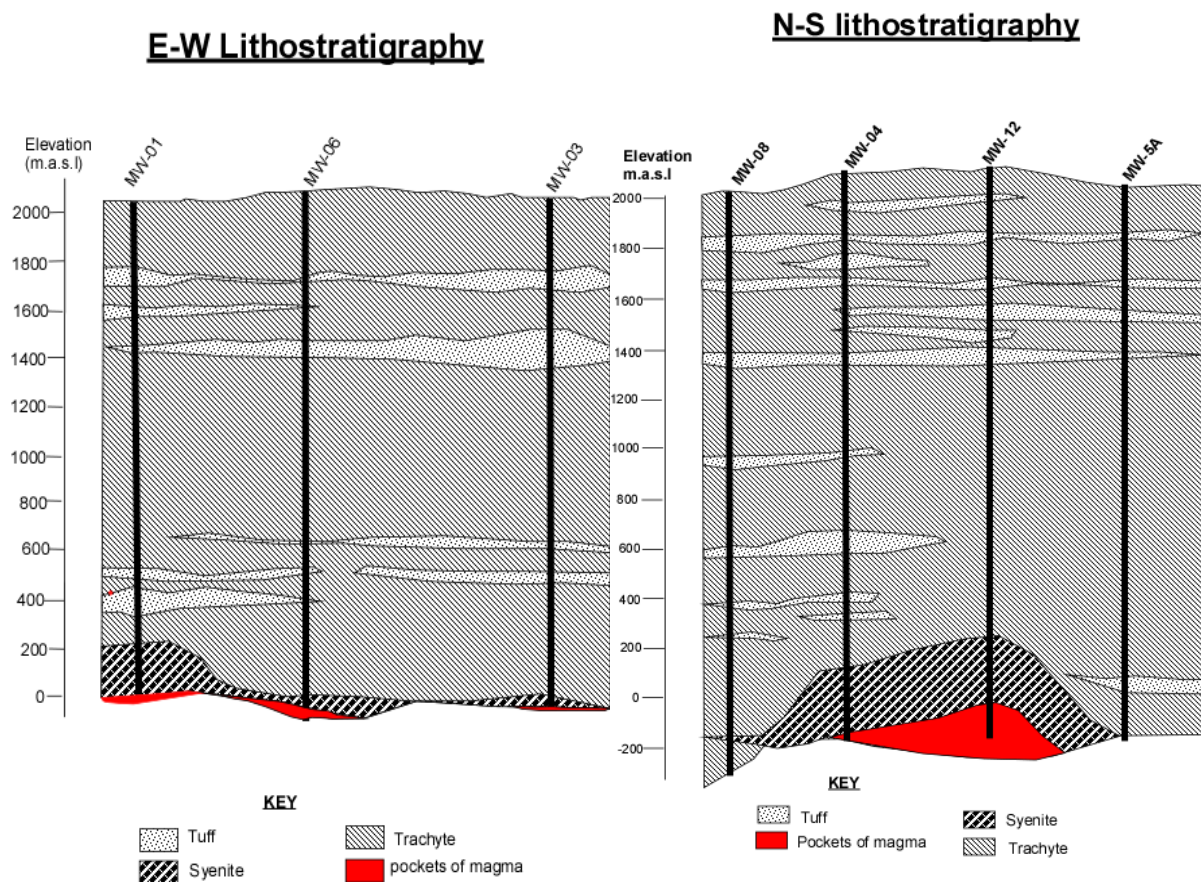
FIGURE 6: Lithological cross-section

2.2.2 Hydrothermal alteration minerals

The main hydrothermal alteration minerals are as described below with hydrothermal mineral cross-section given in Figure 7. There are four alteration zones identified namely; shallower zone is an altered, zeolite-smectite zone, transition zone and illite quartz zone. Magma body is close to well MW-21, MW-09 and MW-19 as depicted in the figure. The high temperature alterations are shallower near the centre of the caldera above the magma hence the doming effect on the alteration zones.

Zeolites
Zeolites are first observed at shallow levels. The types found are cowlescite and the radiating scolecite/mesolite. They occur as vesicle infillings, mostly in the tuff layers of the syn-caldera and post caldera ages. Zeolites are generally thermodynamically metastable at ~<110 °C.

Pyrite
Pyrite is a cubic mineral with a metallic lustre and sometimes the yellowish gold colour is more pronounced. It is disseminated in the groundmass of feldspars. It is encountered almost throughout the well depth but it is most abundant between 1000-1500 m in the most wells and even deeper where intrusive with fracture permeability have been encountered for example in well MW-19. It is an indicator of permeability whereby interaction between the geothermal fluids rich in H_2S has been on-going for a period of time.

Albite
It occurs as an alteration mineral from feldspars. Albite alteration occurs around 500 m but extensive albitization is at from 750 m in many wells within summit area. They become more pronounced within the summit area due to extreme temperature from shallow magma body within this zone.
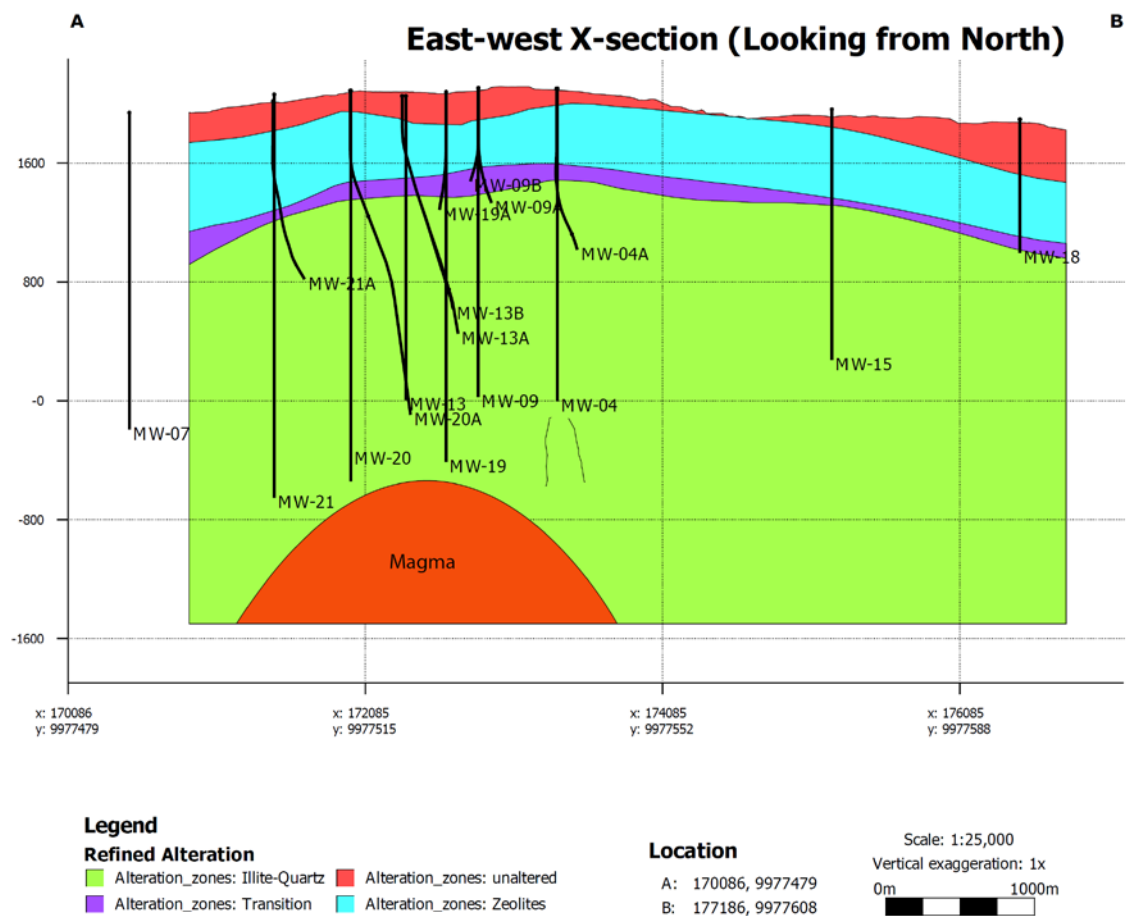
FIGURE 7: Hydrothermal alteration cross-section

Epidote
Analysis of cuttings indicated that epidote is actually rare in many wells within the summit area. However Epidote has been encountered at sometimes very deep levels e.g. at 1956 m in well MW-04 and at 1100 m, 1460 m and 1970 m in well MW-05 based on thin section analysis. Epidote could be rare within summit area due to a shallow degasing magma body. As you move away from summit to well MW-11 epidote became common and abundant and this may indicates less CO_2 gasses and therefore deeper magma body away from summit area. This is further confirming by well MW-19 which was drill to below 2400 m, a depth that was before thought to be magma level.

Clays
XRD analysis previously indicate that there is very little amount of clays in Menengai. Illite is the most common clay followed by smectites at shallow levels above 400 m. More data has shown however that as you move away from magma body clays become abundant, a good example is amounts of clays encountered in well MW-11 Therefore the system within the summit may be younger and thinner.

Calcite
It occurs as dissemination in the groundmass and can be detected by the use of hydrochloric acid (HCL) in the initial analysis. It occurs intermittently throughout the wells. It is very abundant sometimes at deeper levels especially after encountering the intrusive s at around 1900m. This may indicate boiling in these zones.

Quartz
Secondary quartz was found below 580 m and persists almost to the bottom of in many wells. At shallow depths secondary quartz was identified as a replacement to chalcedony while at deeper depths they

deposited in vugs. Quartz is a hexagonal mineral, stable in geothermal systems above 180°C. At summit the quartz isograd forms mild dome being shallow at summit area.

Wollastonite
It is an alteration mineral often associated with contact metamorphism and therefore its occurrence is probably related to the numerous intrusions in the caldera summit area. It occurs at 1544 m to 1824 m in many wells within summit area. It is colourless and fibrous under the binocular microscope and indicates temperatures of 270°C.

Actinolite
This is an alteration mineral classified in the asbestos (amphibole) mineral group. It is high- temperature mineral, forming greenish radiating, acicular crystals or massive to granular aggregates in the groundmass. It is formed by the replacement of ferromagnesian minerals. Actinolite appeared mainly at the intrusive zone in many wells within summit area however it occurs at greater depths away from the caldera centre.

2.2.3 Stratigraphic model
Figure 8 below shows a stratigraphic model as described in text here. The borehole geology data shows that Menengai is predominantly trachytic with intercalation of tuff lenses as is clear in Figure 8.The contacts between different kava flows and within tuff intercalations are the major permeability resulting in aquifers. Magma is very shallow in Menengai especially at the caldera summit where magma is encountered at approximately 2 km, above this hot magma is a thick zone of syenite forming the roof of magma body. The syenite is former magma body that has cooled over time.
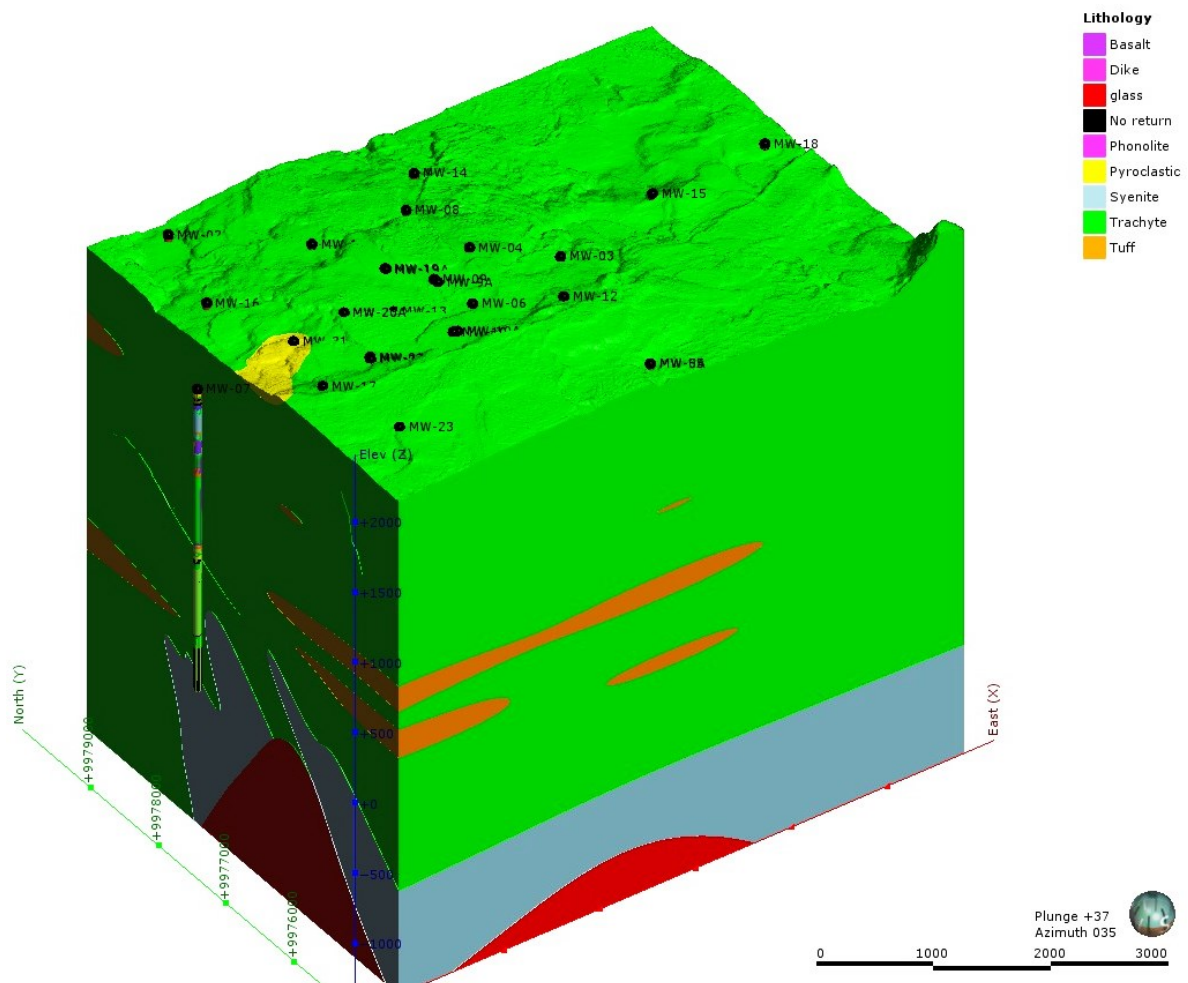

FIGURE 8: 3D Stratigraphic model for Menengai

2.2.4 Alteration model

The alteration model is as highlighted in Figure 9. The shallower depths is the unaltered zone , at slightly deeper depth is a somewhat thicker zeolite zone .The reservoir regions are with the illite -quartz zone which is separated by thin transition zone from the zeolite zone. The illite-quartz zone is bigger and horsts the reservoir and the magma zone. There is doming within the centre indicating shallower reservoir depths within the centre of the caldera above the region where shallow magma body is located.
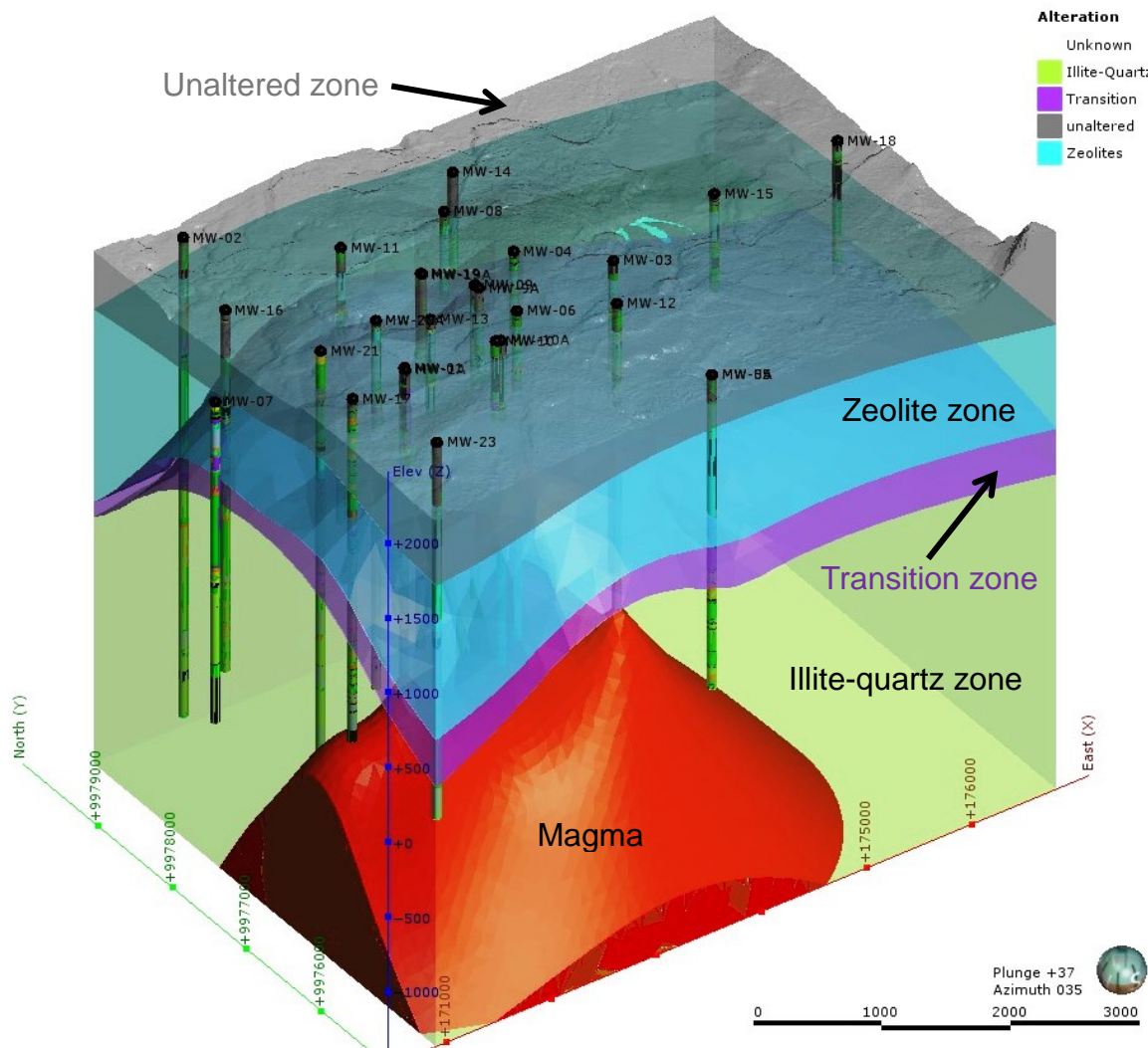
FIGURE 9: 3D alteration model for Menengai

3. MEASURED TEMPERATURES

Contours developed from the measured temperatures and slice d at different depths using voxler software (Figures 9, 10, and 11) demonstrations that the minimum temperature is 27°C in well MW-02 while the maximum temperature was in excess of 390° C measured at the bottom of wells MW-06, MW-04, MW-12 and MW-21.Considering the Iso-maps at 400 m deep, temperatures of around 100°C. Further below the surface temperatures increase in the wells around the centre /summit area. At 700 m deep temperatures of above 210° C are achieved in the wells at the central zone further down a particular high temperature zone is evident taking NNE orientation. This can be interpreted from structural geology as the young structures of the Solai TVA forming a major control for the geothermal system.
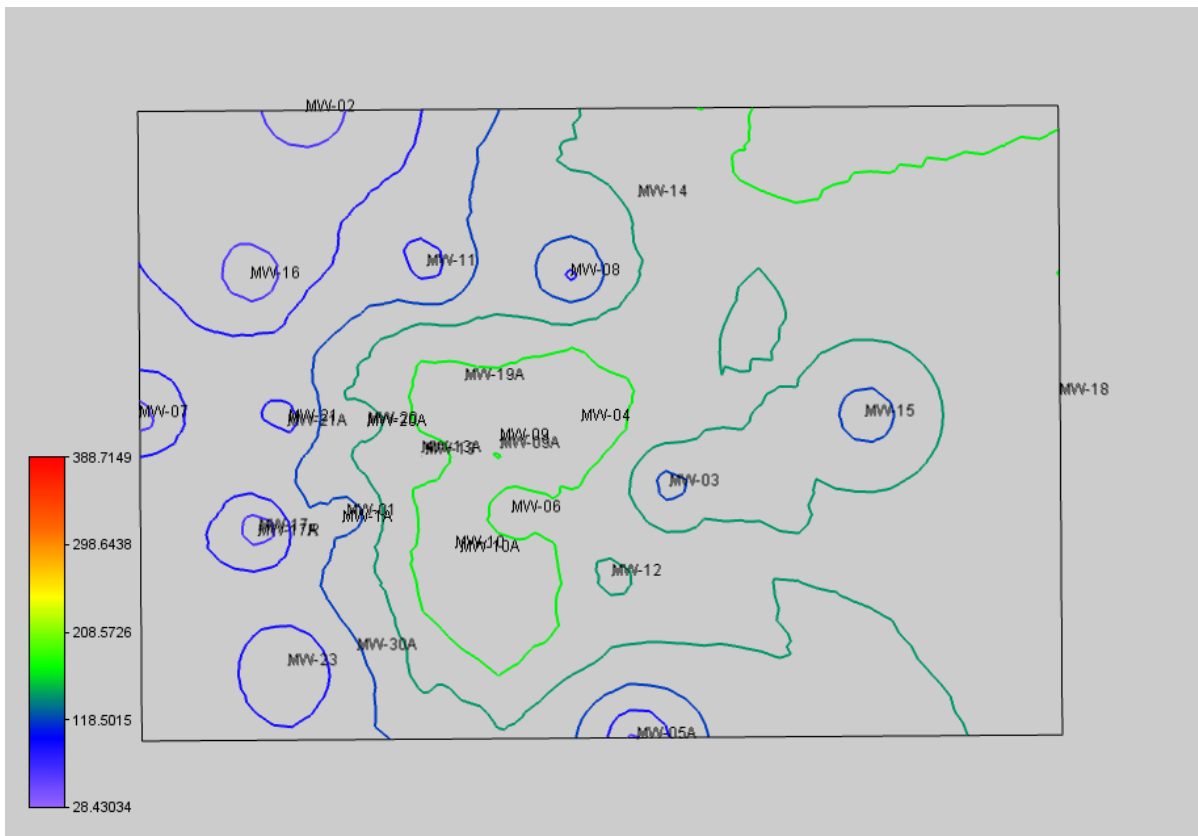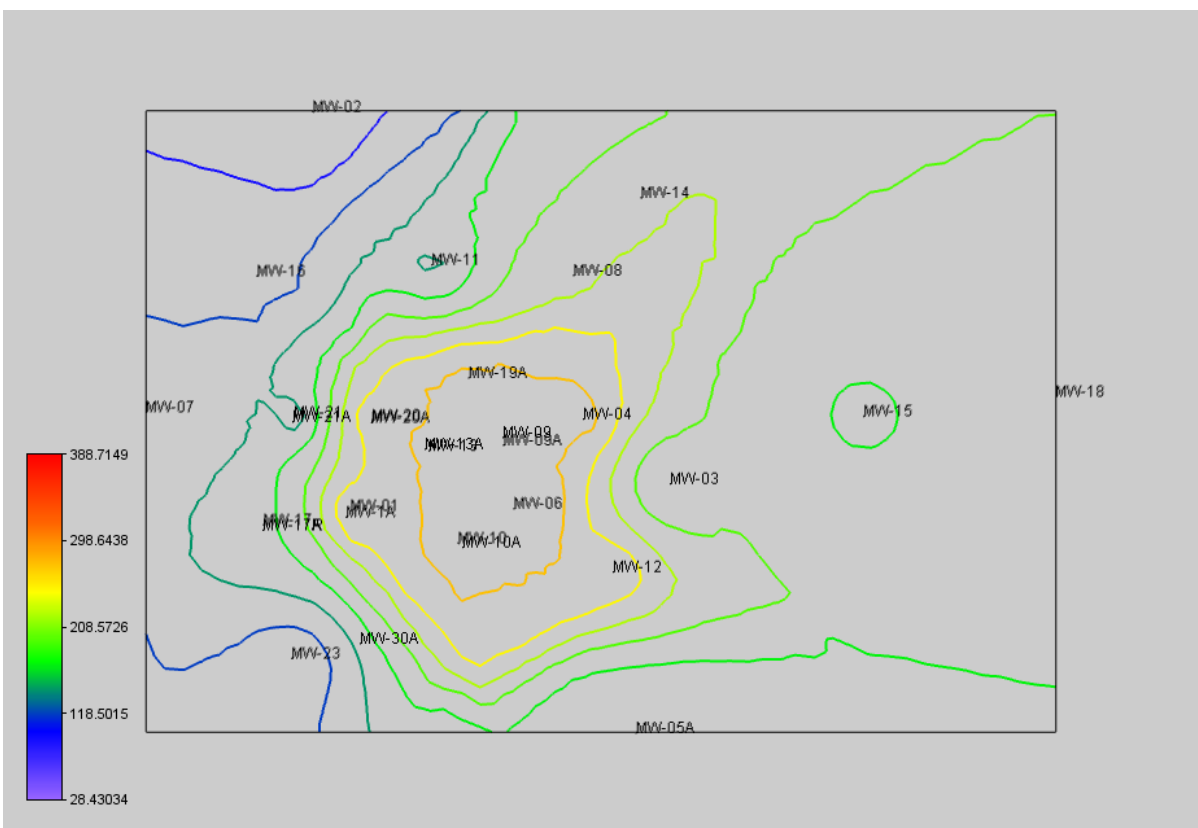
FIGURE 9: Iso- map at 400 m deep
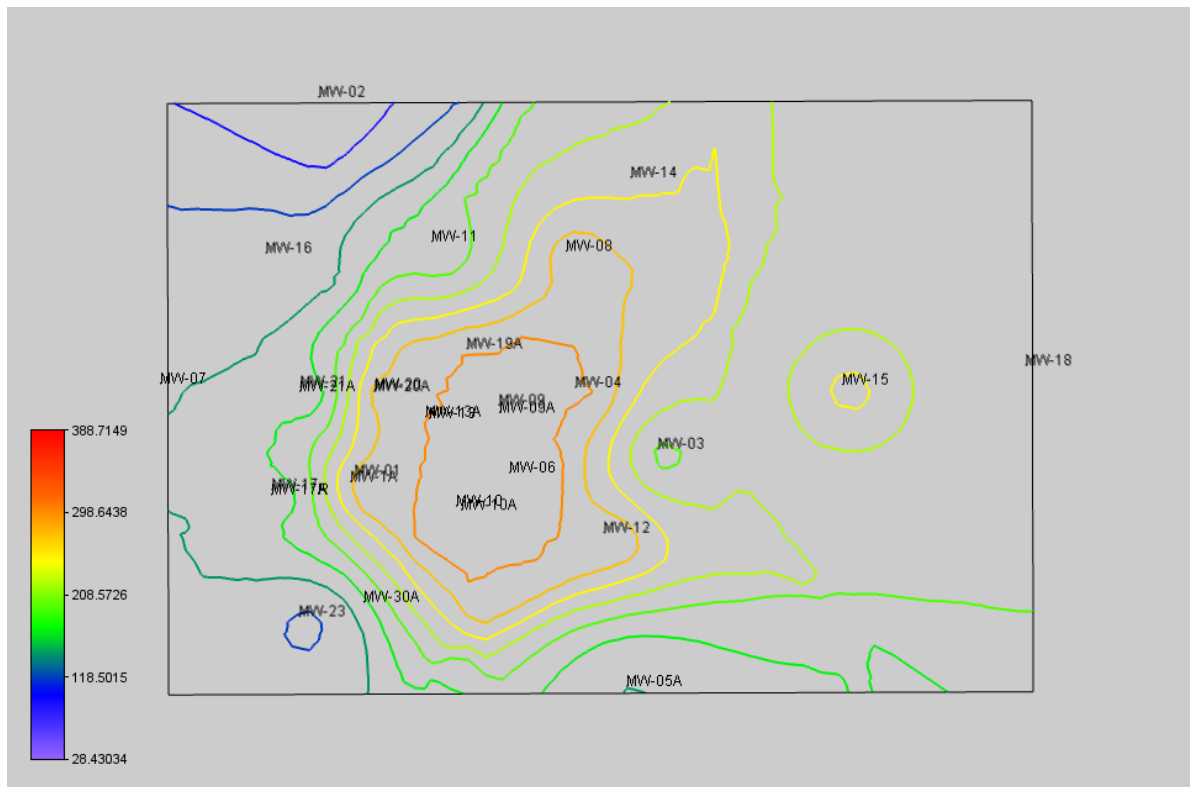

FIGURE 10: Iso-map at 1200 m deep

FIGURE 11: Iso-map at 2000 m deep

3.1 3D temperature model

More than thirty wells have now been drilled within Menengai, in this regard useful temperature data has been obtained. The temperature data has helped in the generation of formation temperatures which were subsequently plotted in leapfrog program. The 3D temperature model resulting from this is as highlighted in Figure 12. It is very clear that within the central area of the caldera high temperatures are experience at shallower depth probably due to upwelling of steam. The central area is locality where the shallow magma body was encountered.

4. GEOCHEMISTRY

4.1 Soil gas survey

The soil gas method is used to infer the geological structures based on the concept that geothermal gases can emanated through subsurface fractures and faults. The proportions of non-condensable gases emitted from manifestations (fumaroles, steam vents, hot springs) generally resemble those in underlying reservoirs, and for volcanic systems, CO_2 is highly emitted as compared with other gases (Goff & Janik, 2000). Faults and fractures favour gas leaks because they increase rock and soil permeability thus the presence of linear soil-gas anomalies longer than several meters are often taken as strong evidence of tectonic features (Fridman, 1990). Radon and carbon dioxide gas in soil have been used in geothermal exploration in different parts of the world (Chiodini et al., 1998; Magaña et al., 2004; Fridriksson et al., 2006, Voltattorni et al, 2010). CO_2 is known as one of the volatiles emanating from magmatic processes. In Menengai high carbon dioxide concentration in the soil gas (Figure 13) was observed around north east of the caldera and in the north western (Ol' rongai) areas. Other areas west of the caldera exhibits high concentration as well as patches to the north, east and south close to the caldera rim. The high CO_2 levels generally coincide with deep-seated faults or fractures.
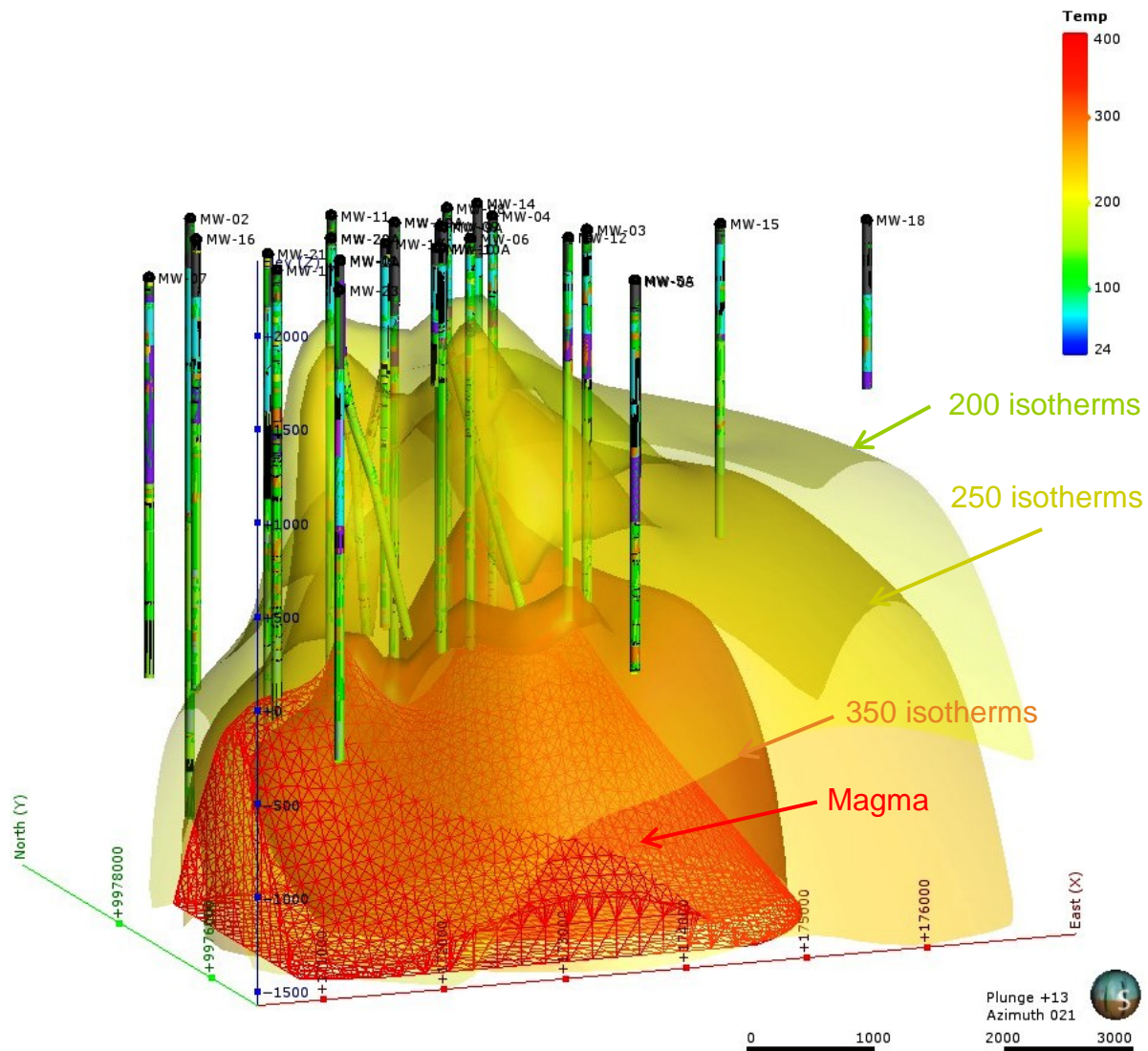
FIGURE 12: 3D temperature model for Menengai

4.1.1 Radon distribution in the soil gas

The areas with high concentration of Rn-222 are indicative of areas of high permeability and high heat flow as shown by coincidence with the manifestations in the central, north and northeast parts out of the caldera (Figure 14). Other areas are in the eastern part of the caldera rim.

4.2 Fumarole chemistry

Hydrothermal activity is manifested in the Menengai volcano area by the occurrence of fumaroles and altered rock/grounds. Fumaroles (Figure 15) are located mainly inside the caldera floor. Three groups of active fumaroles found in the caldera have an aerial extent ranging from a few m^2 to less than a km^2. The two groups in the central and western portion of the caldera floor are located within fresh lava flow and close to eruption centres. The other group of fumaroles located in the central eastern part of the caldera floor is found at the young lava/pumice contact and has extensively altered the pumice formation. The structural controls for these groups of fumaroles appear to be the eruption craters that may be the source of the pyroclastic deposits. Geothermometry results are as highlighted in table 1, the reservoir temperature range from 276-352° C which pretty much were confirmed by the measured temperatures after drilling of the current wells in Menengai.
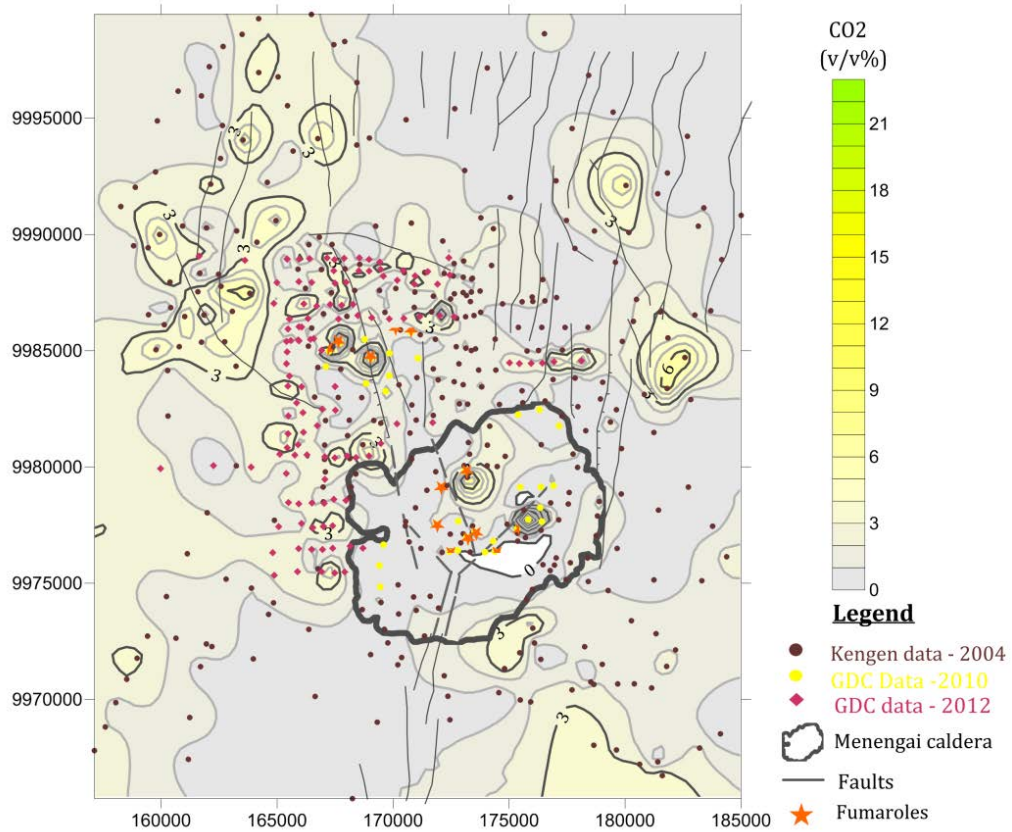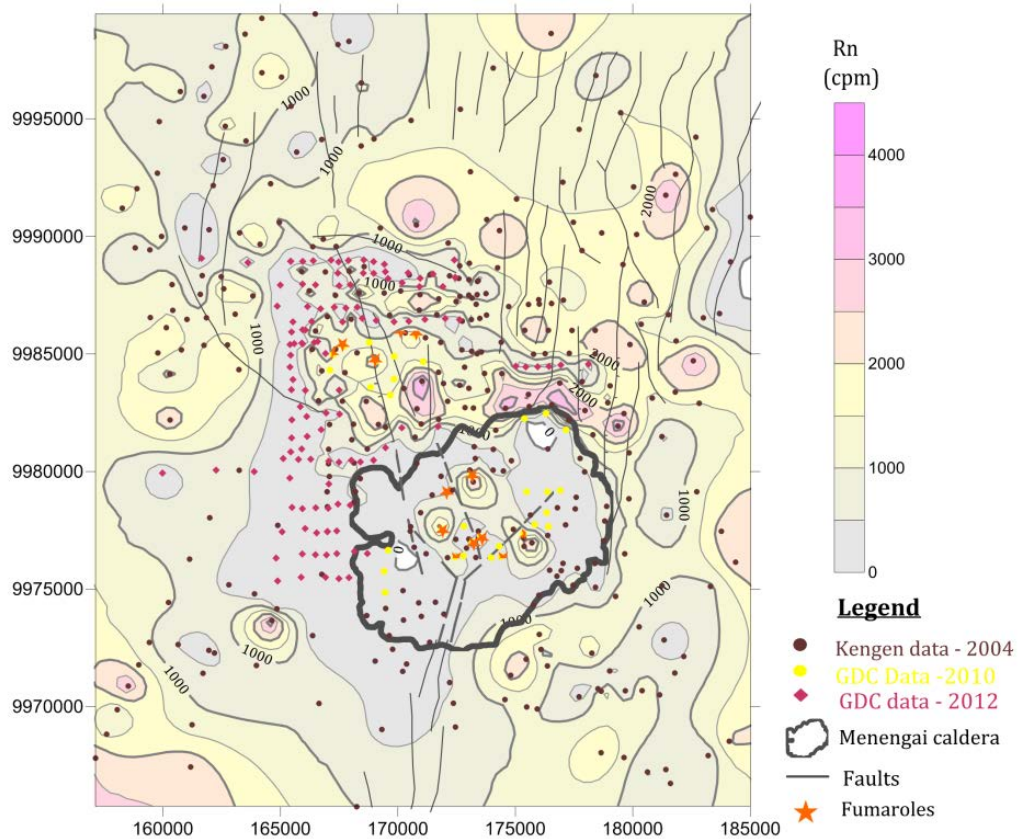
FIGURE 13: CO_2 distribution

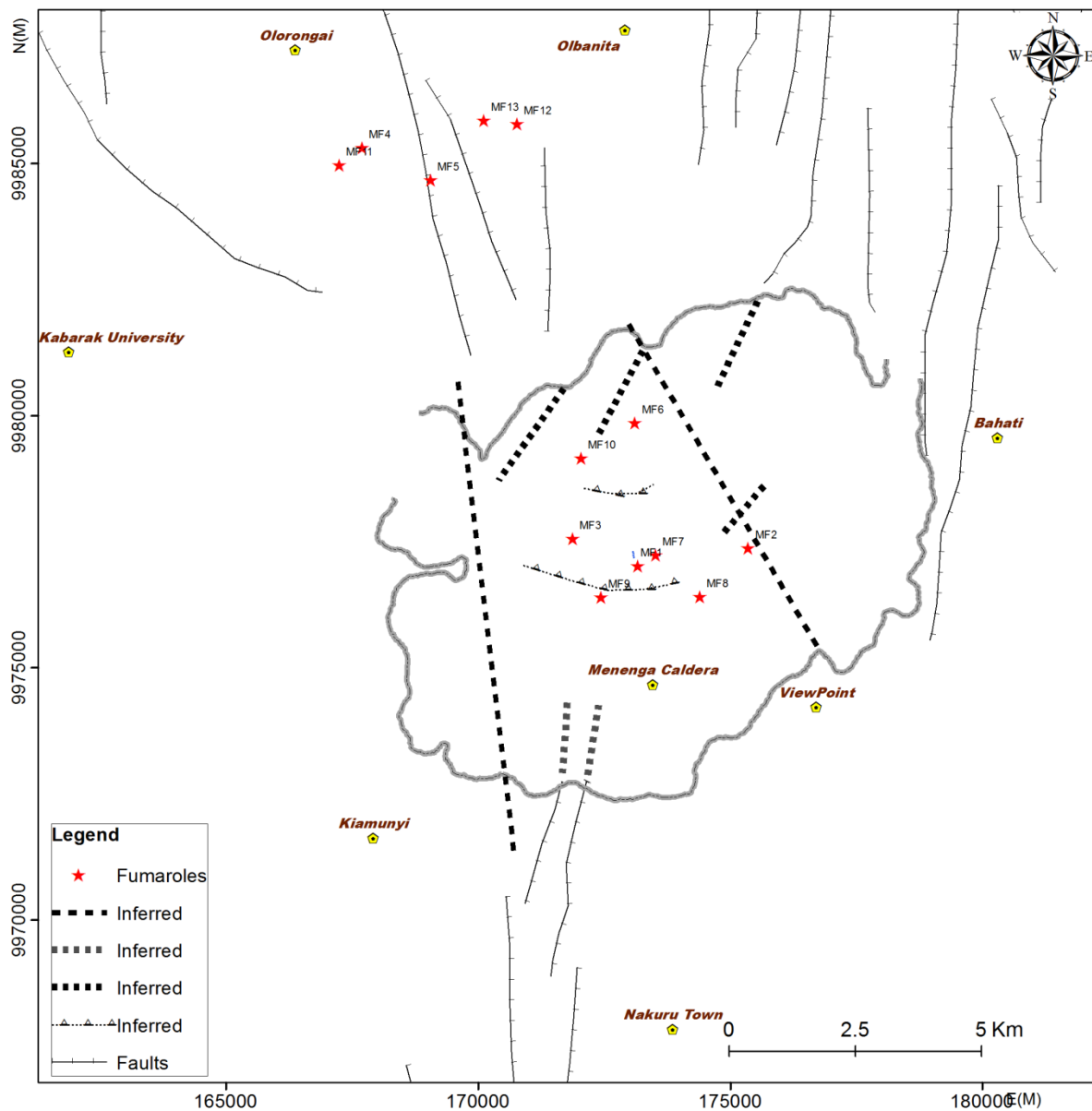FIGURE 14: Radon (222 Rn) and distribution

FIGURE 15: Location of fumaroles

4.3 Geothermal well chemistry

The well discharge chemistry is displayed here using few wells but gives the general picture of the Menengai reservoir fluids. Wells MW-01, MW-03, MW-04, MW-06, MW-09 and MW-12 data are described below. The wells sampled had varying sampling pressures that were in tandem with the wellhead pressures as shown in Figure 16.

4.4. Fluid chemistry

The fluid encountered in Menengai wells are summarized by the results from a few wells. The fluids are of Na-HCO$_3$ type and high in pH (Figure 17 and 18) with concentrations of over 1000 mg/kg of chloride reported in well MW-04. The high pH, (pH range of 8-10), can be attributed to the high bicarbonates and CO$_2$ gas that exsolves as the fluid boils and moves towards the surface. High chloride values (>400 mg/kg) are also detected in the fluids. The Cl and SiO$_2$ values are indicative of hot geothermal fluid entry into the wells (Figure 19).

TABLE 1: Fumarole temperature estimations by geothermometer calculations
(data from Lagat et al., 2010)

Fumarole No.	Location		Sampling temp (°C) *Jan 2010*	Sampling temp (°C) *Dec 2009*	Geothermometry* (°C)	
	Eastings	**Northings**			T_{H2S}	$T_{H2S-CO2}$
MF-01	173170	9977023	70	62	281	276
MF-02	175353	9977375	88	88	293	304
MF-03	171876	9977567	85	85	262	247
MF-06	173112	9979852	75	75	296	302
MF-07	173520	9977240	88	88	327	352
MF-08	174395	9976411	88	88	295	299
MF-09	172441	9976400	-	70	279	274

* Geothermometric calculations

a. T_{H2S} - Arnórsson and Gunnlaugsson (1985)

b. $T_{H2S-CO2}$ - Nehring and D'Amore (1984)
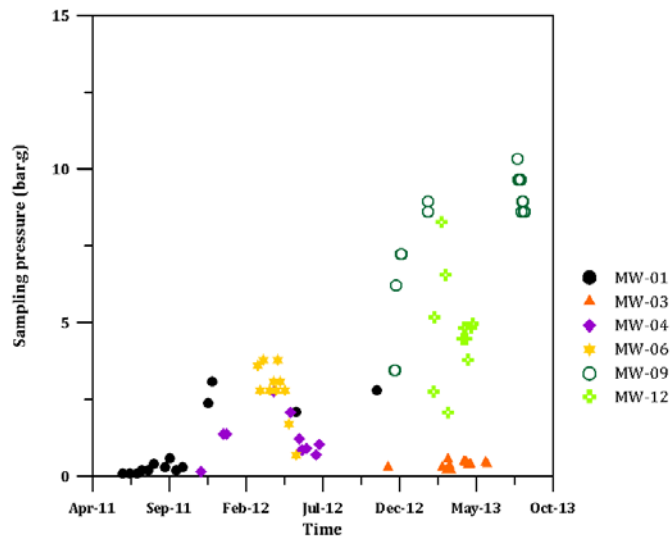
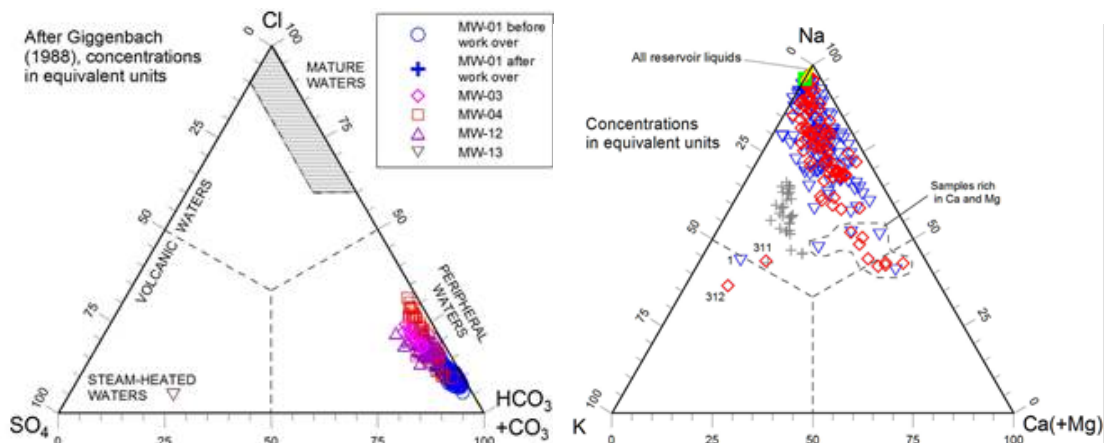FIGURE 16: Variation of the well sampling pressures
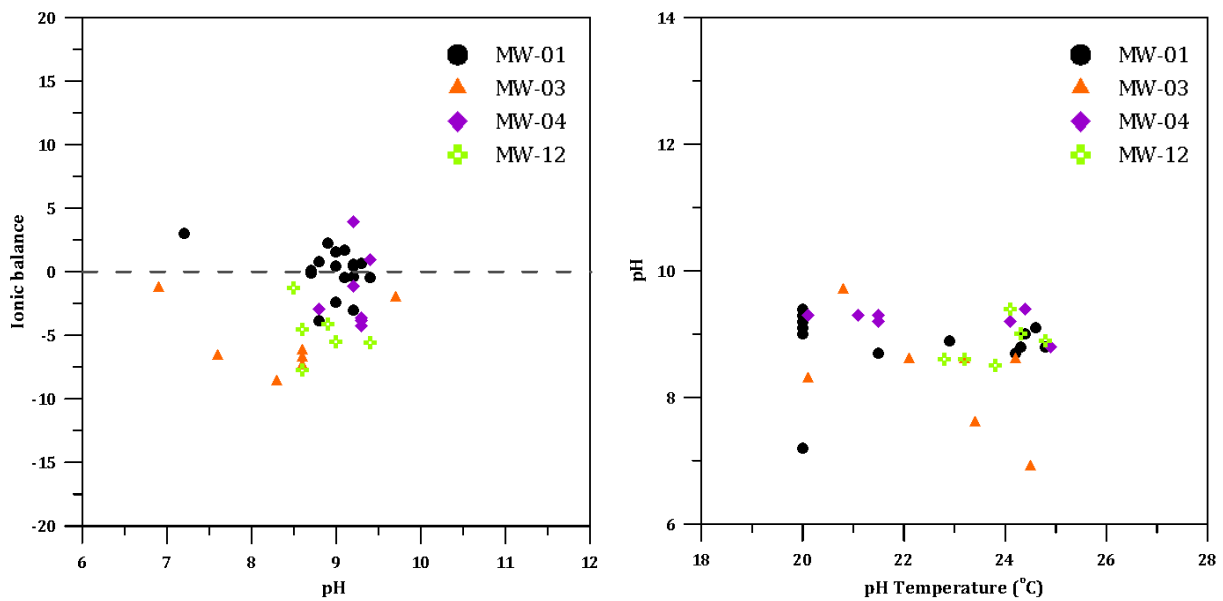

FIGURE 17: Na-HCO₃ type fluids

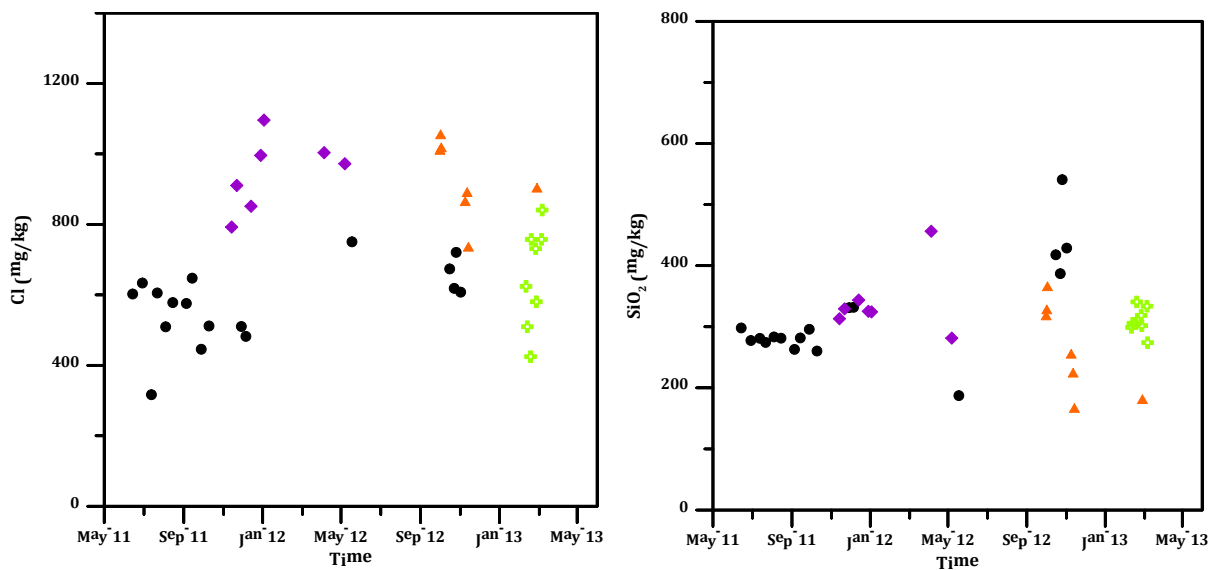FIGURE 18: Ionic balance and pH of two phase discharges from Menengai wells

FIGURE 19: Chloride and silica concentrations of Menengai wells at 5 bar-g. Symbols as in Figure 18
Geothermometric temperatures calculated from minerals (SiO$_2$) and gases (CO$_2$, H$_2$S and H$_2$) give
temperatures in the range of 180 – 330 °C (Figure 20). The temperatures however vary per well, an
indication of more than one major feed zones contributing fluids of different elemental compositions
and temperatures. This can be verified from the measured temperatures per well from the reservoir
well logs.

4.5 Gas chemistry

Menengai wells indicate high gas (NCG) content, predominantly CO$_2$ which is above 2000 mmol/kg in
MW-01, MW-03, MW-04, MW-06 and MW-12, the maximum discharges being observed in MW-01
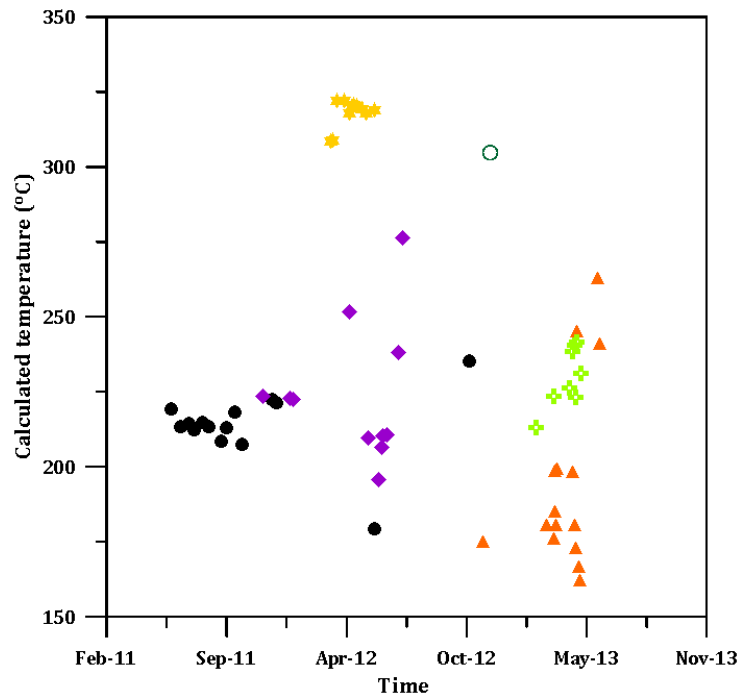after rig work-over cleaning in 2012 (Figures 21 and 22).

FIGURE 20: Reservoir temperatures calculated from quartz geothermometers (two phase wells) and average of CO_2, H_2S and H_2 geothermometers (one phase wells). Symbols as in Figure 18.
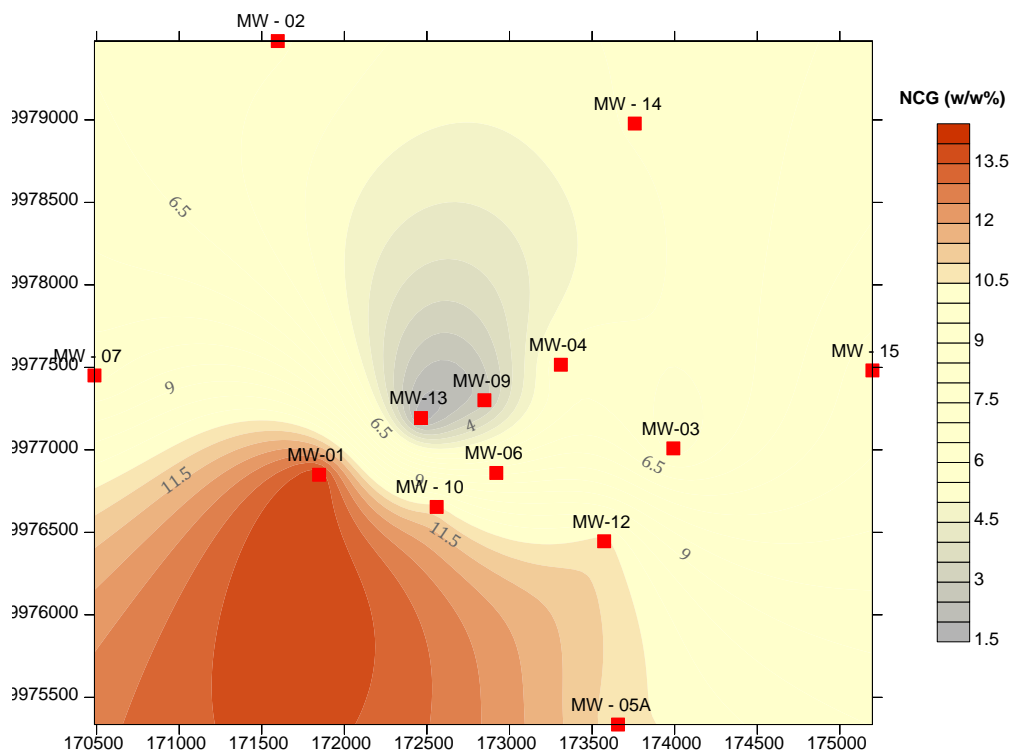

FIGURE 21: Non condensable gas (NCG) distribution in Menengai wells
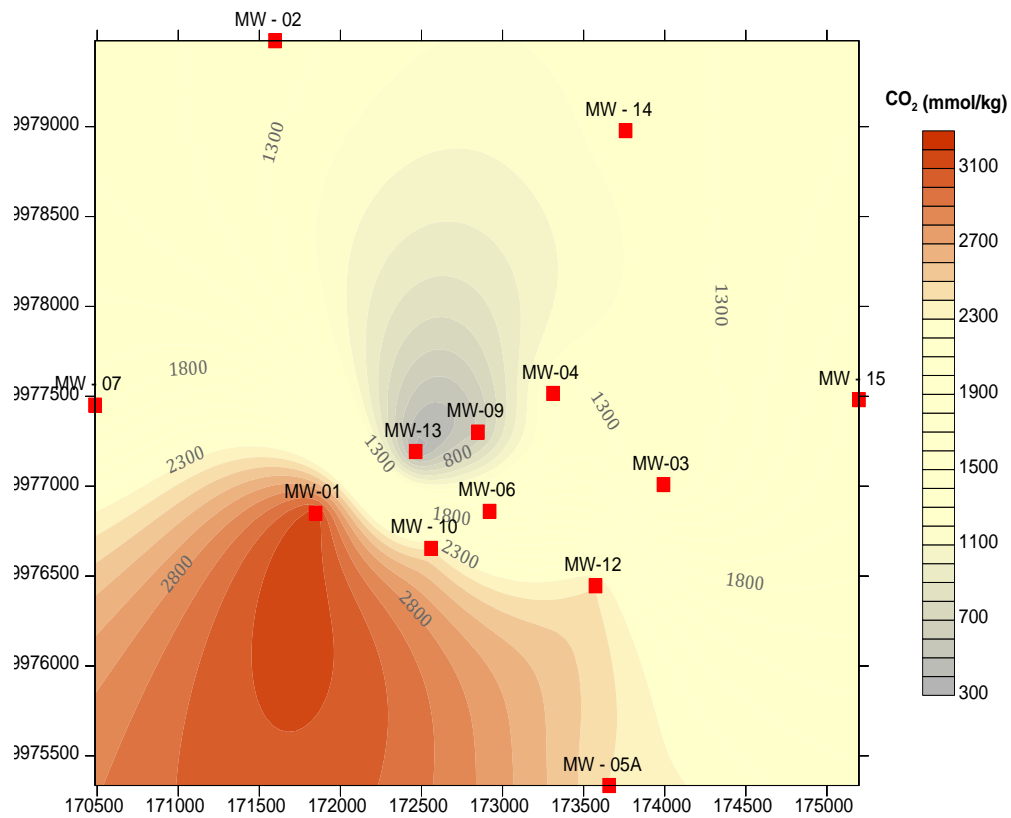
FIGURE 22: CO$_2$ distribution in Menengai wells

High H$_2$S, >30 mmol/kg is observed in MW-04, MW-06, MW-09, MW-10 and MW-12 with a maximum in MW-06 (Figure 23).These gases should typically show somewhat a pattern (Scott et al., 2011) but
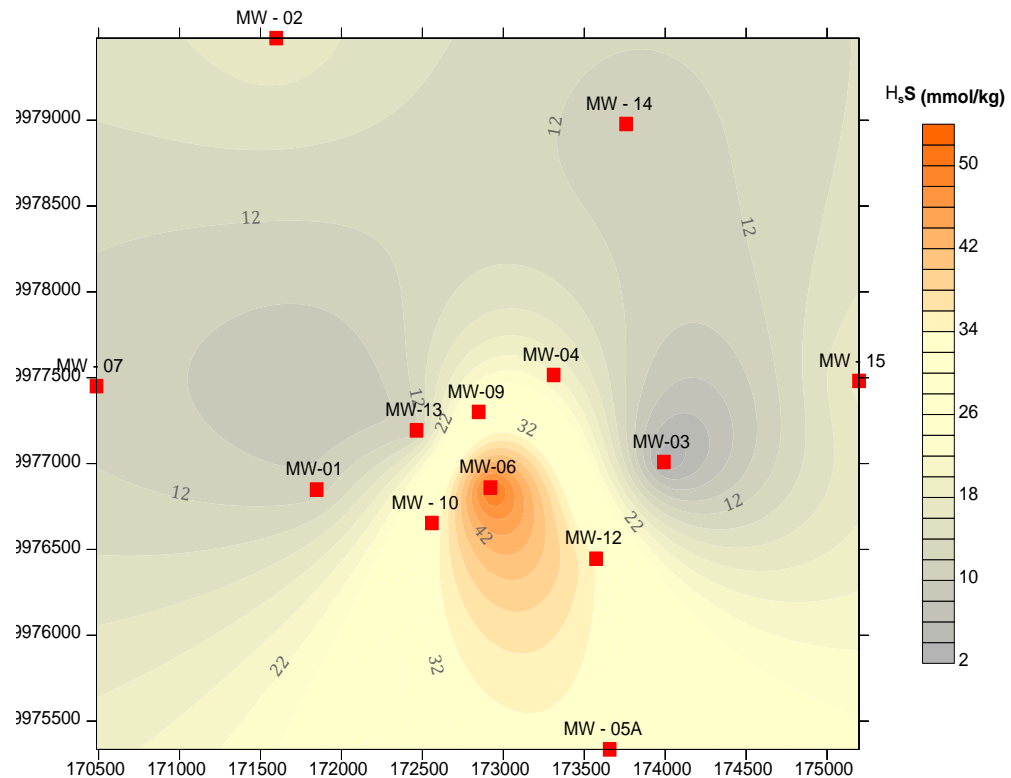

FIGURE 23: H$_2$S distribution in Menengai wells

the differences here are intriguing and could be due to shallow magmatic body / heat source around the summit area than what is normally observed for mineral-gas equilibrium controlled geothermal environments. This can also be compared to the geothermometers where the calculated temperatures and the measured temperatures vary in this case; the measured temperatures (T meas.) are much greater than the calculated temperatures (T quartz) for at least the two phase discharging wells (see the reservoir evaluation of measured temperatures). Truesdell and Fournier 1977 made comparisons of the measured and the calculated temperatures and concluded that equilibrium is only observed in the well if all the temperatures are closely related or equal i.e. T meas. = T quartz.

The gas content of the steam samples depends on the original gas content of the reservoir water, the enthalpy of that water, possible loss/gain of steam during flashing underground and the sampling pressure. Generally, the relative abundance of CO_2, H_2S and H_2 in geothermal fluids will depend both on the fluid type (dilute/saline) and temperature (Arnórsson, 1986; Nicholson, 1993). The effect of temperature on the concentrations of these gases in Menengai is evident in Figure 24 describing the temperature dependence of the gases. However, CO_2 concentrations do not show a clear relationship with temperature, except what is observed in well MW-03 compared to MW-09, MW-13 and to some extent, MW-04. Arnórsson (1986) observed that the relative abundance of CO_2 is high at temperatures below about 250°C but decreases with increasing temperature until at about 300°C, when it starts with increasing temperature until at about 300°C, when it starts to increase again.
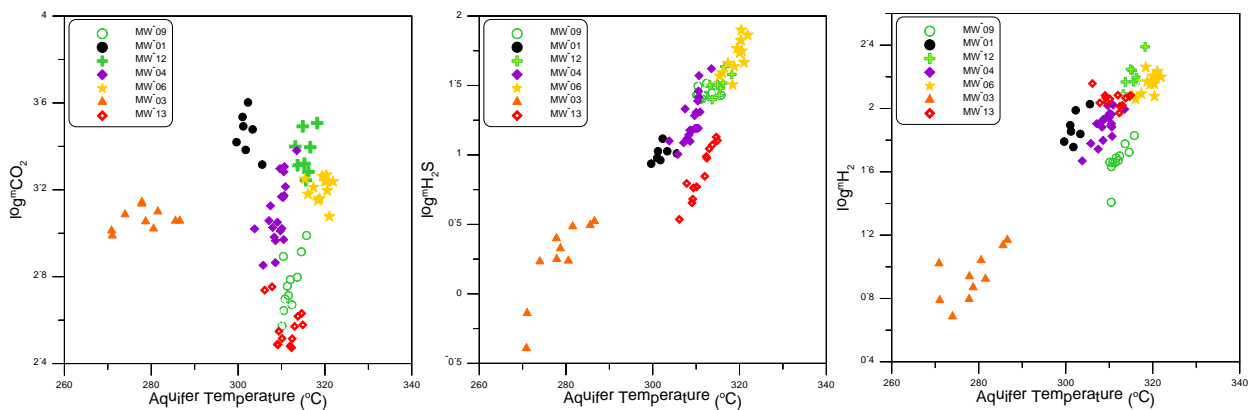

FIGURE 24: The concentrations of CO_2, H_2S and H_2 versus temperature in the geothermal wells in Menengai. Aquifer temperature used is the average of CO_2, H_2S and H_2 geothermometer temperatures by Arnórsson and Gunnlaugsson (1985).

5. GEOPYHSICS

5.1 Resistivity

Cross section through the centre of Menengai caldera shows a thin high resistivity (> 70 ohm-m) which is the top layer of the fresh fractured lavas. It is underlain by a thick low resistivity (30 ohm-m) layer defining the reservoir zone. Resistivity of (< 10 ohm-m) to the west is pyroclastics. The top of the system usually defined by a low resistivity is virtually non-existent in Menengai. At about 500 masl the reservoir zone (30 ohm-m) is intruded by a high resistive vertical elongation (100 ohm-m), interpretations for this is still not conclusive (Figures 25-27).
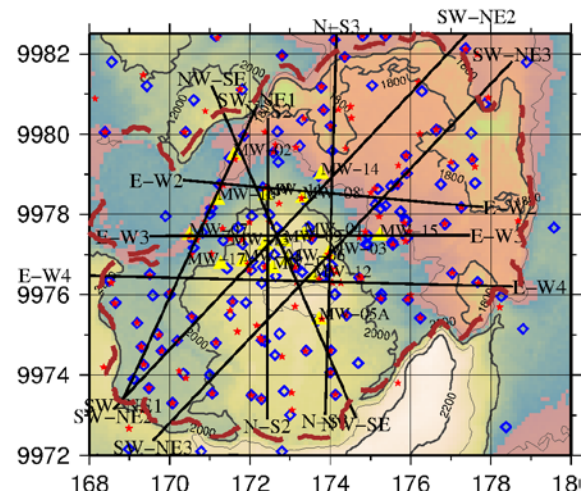

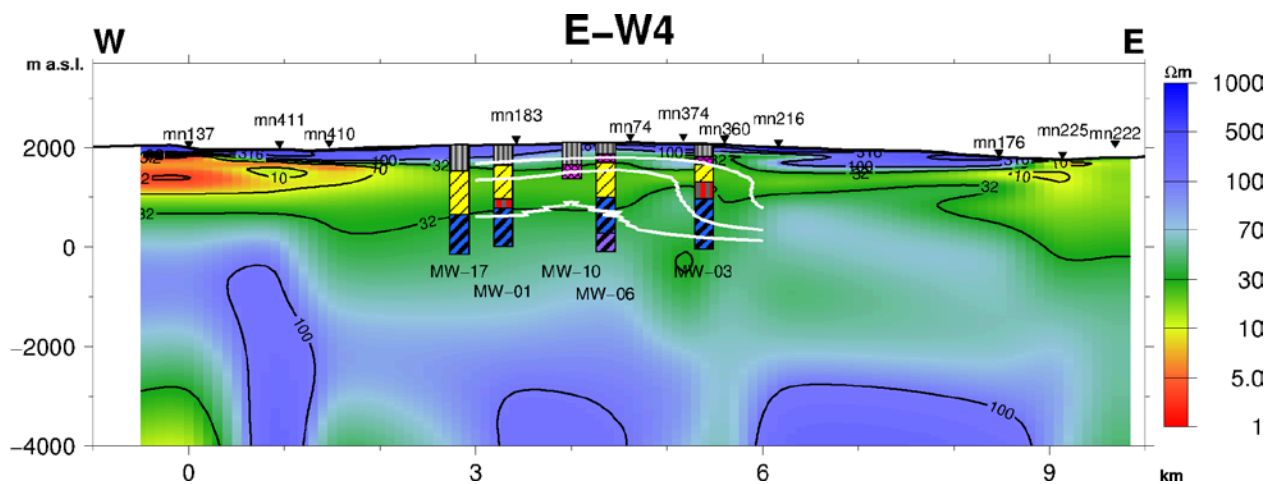FIGURE 25: Resistivity profiles in the Menengai caldera
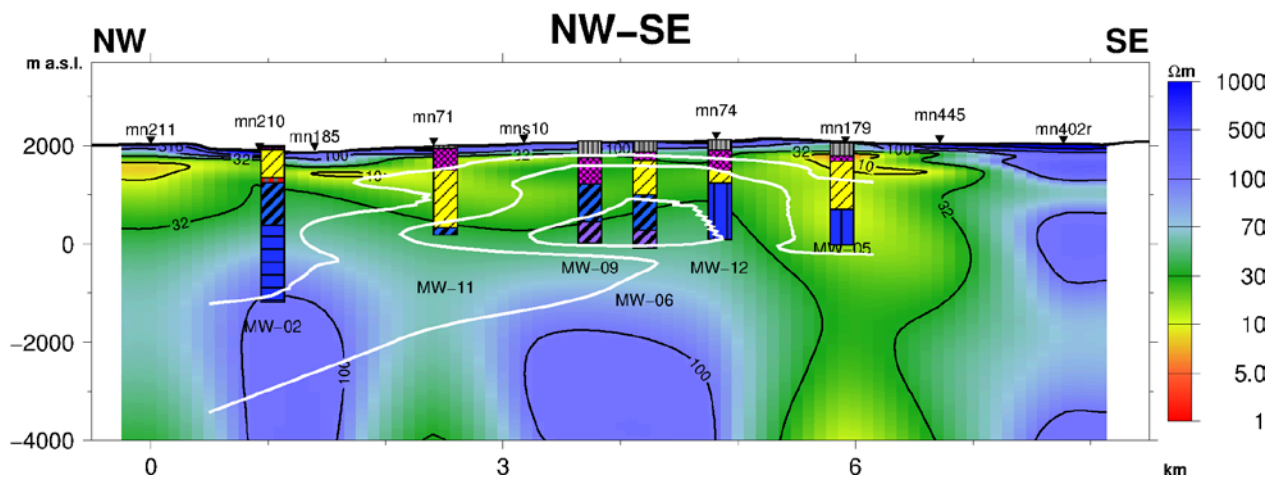
FIGURE 26: 1-D E-W4 MT resistivity cross-section

FIGURE 27: 1-D NW-SE MT resistivity cross-section (GDC, 2014)

5.2 Gravity

Recent campaign of data collection by the GDC within the Menengai caldera has resulted in a total of 60 stations were collected. Figure 28 is a map showing the recently done profiles.

5.2.1 Data processing

The previous and recent data set of gravity was used to develop a Bouguer anomaly map of Menengai caldera (Figure 29). The map shows gravity high at the centre of the caldera confined by gravity lows to the north, east and south. The anomaly may infer an intrusion and this may be the magmatic body encountered during the well drilling.

5.3 Seismic data

Simiyu (2009) defined a shallow magma body at the centre of the caldera evidence by intense, smaller and shallower micro-seismic activity this is vice versa towards the periphery. Additionally Ray paths from deep events through the centre of the field show that there is a deep attenuating body directly beneath the central part of the caldera structure and taking on geometry with a NE-SW (Figures 30 and 31).
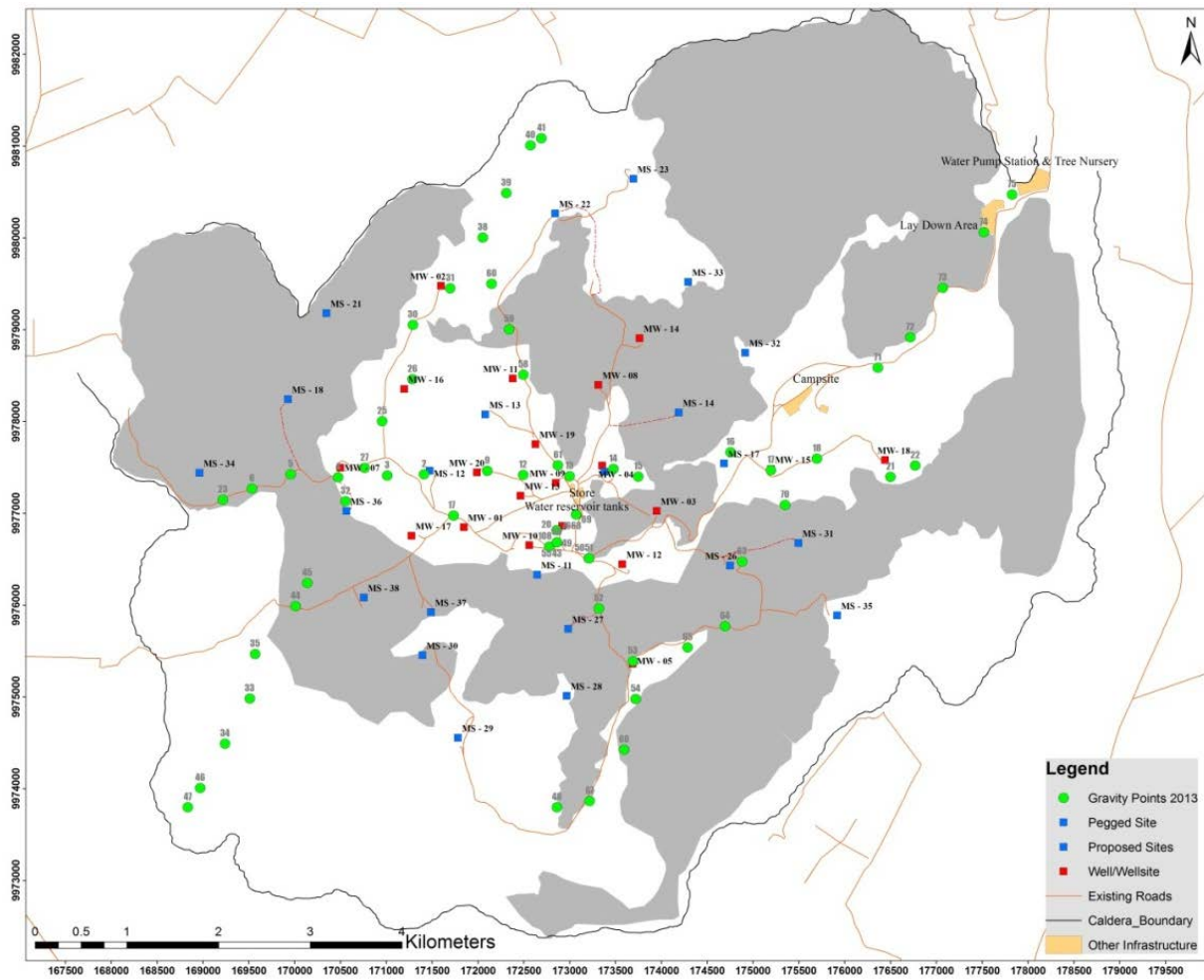
FIGURE 28: Map showing gravity profiles done (Green circles) in Menengai caldera
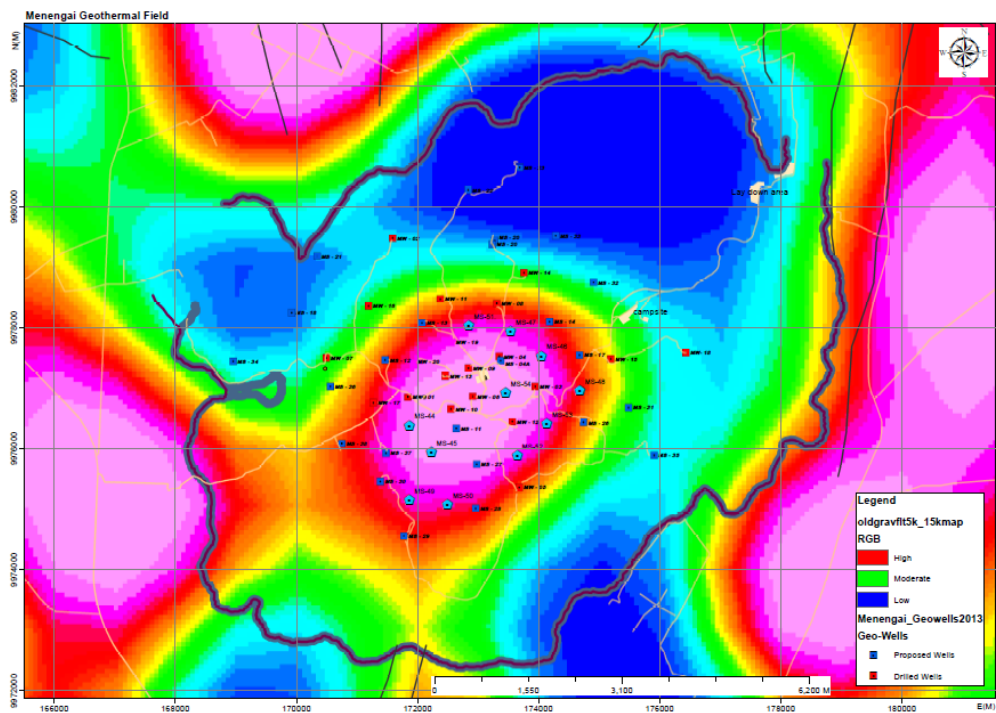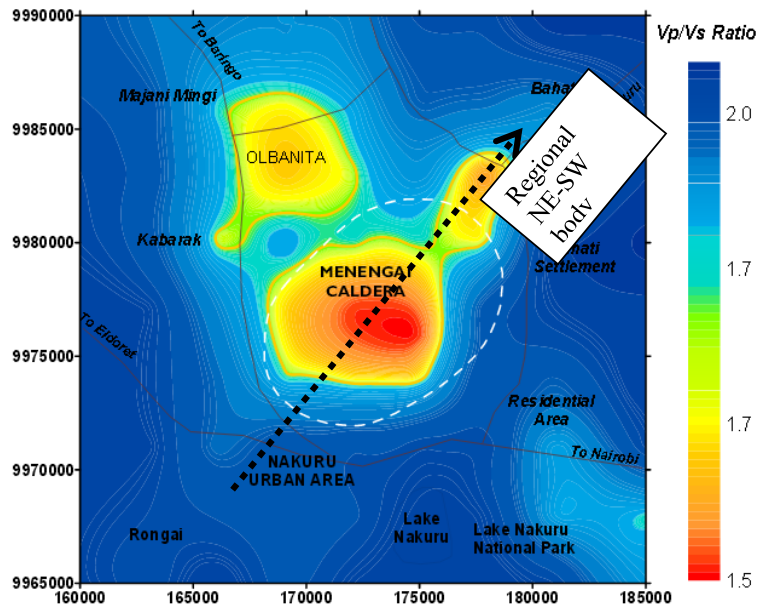

FIGURE 29: Bouguer anomaly

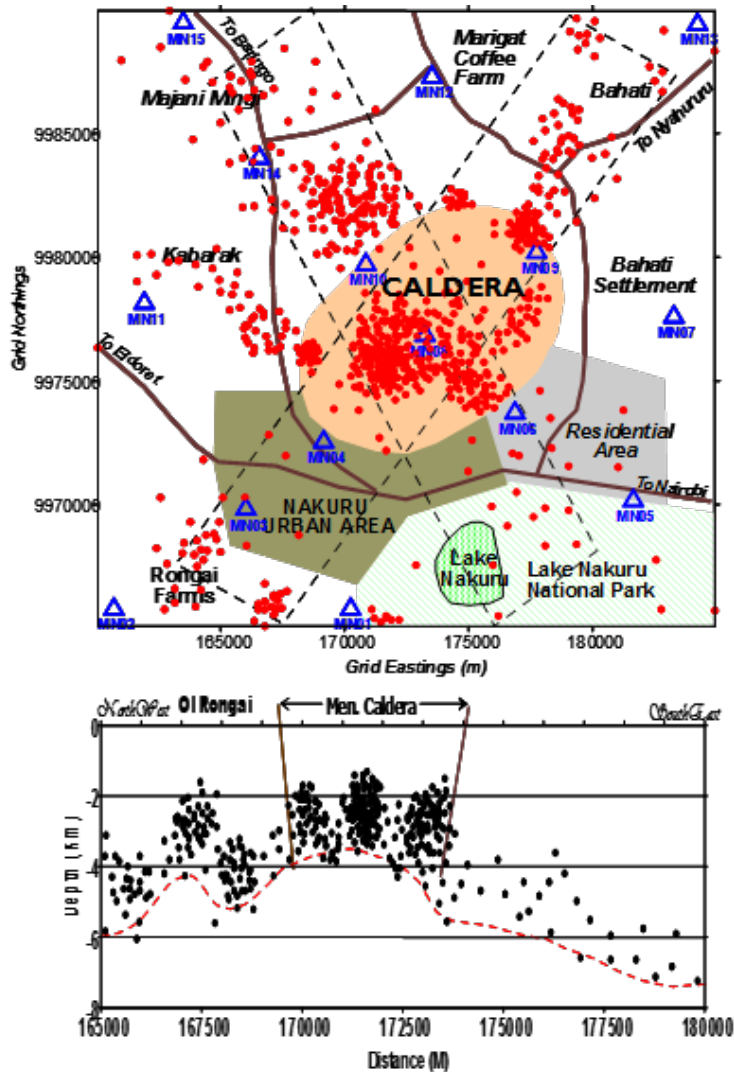FIGURE 30: Regional NNE anomaly from seismic events (Simiyu 2009)

FIGURE 31: Shallow intense seismic events at the centre of the caldera (Simiyu, 2009)

6. DISCUSSION AND CONCLUSION

Surface geology suggests that Menengai has had a recent volcanic activity marked by the lava flow mapped at the central area that issued from the E-W fissure. The south of the caldera has also been active in recent past based structures and evidence of volcanism in this area namely eruption cones, young lava flowing into the caldera from the outer rim. Therefore, the central and south of the caldera are interesting areas for further geothermal exploration. From borehole geology there is a shallow magma at the centre of the caldera, this is heat source driving the system here hence the up flow as inferred from geochemistry located at this zone. The shallow magma is further confirmed by shallow seismic events here, the seismicity infers NNE-SSW shallow magmatic body. Measured temperatures agree with this inferred anomaly from seismic events Presentation the NNE-SSW body that develops as you slice Iso maps from 400 m, 1200 m and 2000 m deep from surfaces. Based on this we can establishes that the NNE-SSW body traces the young structures associated with Solai TVA as controlling structures for the system. The N-S and NNW structures are older and may control a separate system from the caldera system.

The Menengai conceptual model for Menengai field can be summarized as follows:

1. The caldera shape mimics the of magma chamber below i.e. The NNE-SSW orientation;
2. Menengai fluid flow system is NNE-SSW following the Solai TVA (young) structures and possible overlying a magma body of the same shape;
3. The young structures associated with Solai TVA are major controlling structures for Menengai;
4. The Older NNW and N-S structures may be controlling a separate system from caldera system; and
5. Up-flow zone within the central or summit area.

Below is snap shot of the process flow for development of Menengai model using Leapfrog software (Figure 32).
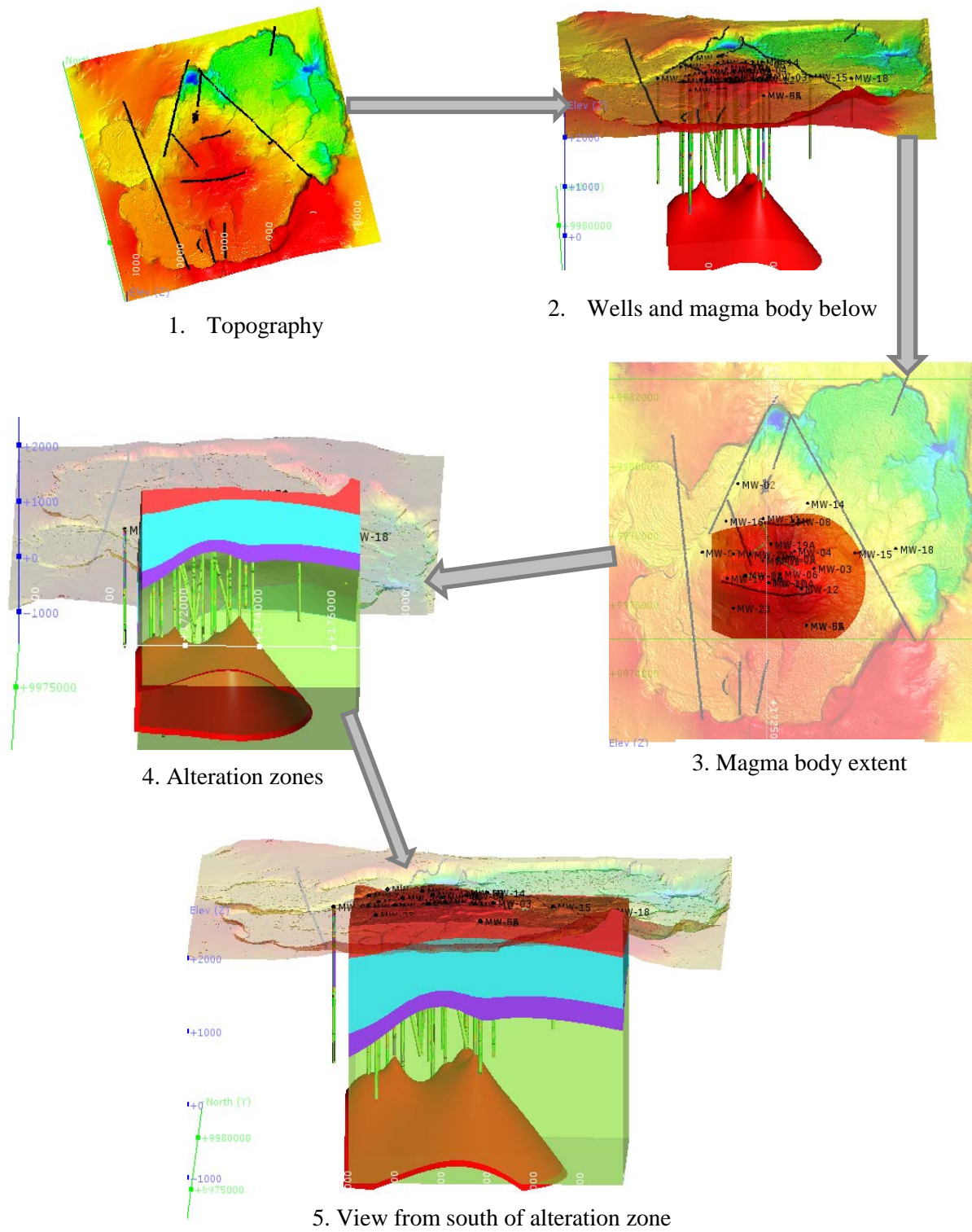
1. Topography

2. Wells and magma body below

3. Magma body extent

4. Alteration zones

5. View from south of alteration zone

FIGURE 32: Leapfrog model process flow

REFERENCES

Chiodini G., Cioni, R., Guidi, M., Raco, B., and Marini, L., 1998: Soil CO_2 flux measurements in volcanic and geothermal areas. *Applied Geochemistry, 13*, 543-552.

Fridman A.I., 1990: Application of naturally occurring gases as geochemical pathfinders in prospecting for endogenetic deposits. *J. Geochem. Explor., 38*, 1–11.

Fridriksson, Th., Kristjánsson, B.R., Ármannsson, H., Margrétardóttir, E., Ólafsdóttir, S., and Chiodini, G., 2006: CO_2 emissions and heat flow through soil, fumaroles, and steam heated mud pools at the Reykjanes geothermal area, SW Iceland. *Applied Geochemistry, 21*, 1551–1569.

Goff, F. and Janik, C.J., 2000: Geothermal systems. Encyclopaedia of Volcanoes. 817 – 834.

Leat, P.T., 1984: Geological evolution of the trachytic caldera volcano Menengai, Kenya Rift Valley. *J. Geol. Soc. London, 141*, 1057-1069.

Magaña M.I., López, D., Barrios, L.A., Perez, N.M., Padrón, E. and Henriquez, E., 2004: Diffuse and convective degassing of soil gases and heat at the TR-6-Zapotillo hydrothermal discharge zone, Berlin Geothermal Field, El Salvador. *Geothermal Resources Council Transactions, 28*, 485-488.

Mibei, G.K., 2012: Geology and hydrothermal alteration of Menengai geothermal field. Case study: Wells MW-04 and MW-06. Report 21 in: *Geothermal training in Iceland 2012*. United Nations University Geothermal Training Programme, Reykjavík, Iceland, 437-465.

Robinson, H., 2015: Conceptual hydrogeological model for caldera-associated high-enthalpy geothermal reservoirs in eastern Africa. PhD thesis, unpublished.

Simiyu, S.M., 2009: Application of micro-seismic methods to geothermal exploration; example from the Kenya rift. *Paper presented at "Short Course IV on Exploration for Geothermal Resources", organized by UNU-GTP, GDC and KenGen*, at Lake Naivasha, Kenya, 27 pp.

Voltattorni, N., Sciarra, A., and Quattrocchi, F., 2010: The Application of soil-gas technique to geothermal exploration: Study of hidden potential geothermal systems. *Proceedings World Geothermal Congress 2010*, Bali, Indonesia, 7 pp.